

AAE 520L  
Lab Team 6  
3/15/2004

AAE 520L  
Experimental Aerodynamics  
Spring, 2004  
Professor: Dr. Schneider  
Teaching Assistant: Chad Vetter

## Lab 2

# Supersonic Shock and Flow Visualization

By  
Lab Team 6:  
Christopher J. Bies  
Geoffrey A. Bixby

**Abstract**

Supersonic flow has long been a complicated and interesting field to study. More specifically oblique shock waves and expansion fans have drastic effects on key aircraft components. Aircraft flaps and engine inlets regularly require the study of supersonic shock theory. The purpose of this experiment was to look at the shock interaction of two ramps that could easily be used to simulate aircraft components such as flaps, elevators, inlets, or countless other components. The two ramps studied were 15 and 25 degree test bodies. A secondary purpose of the experiment was to learn how to instrument and use a supersonic wind tunnel correctly.

Some of the results of the experiment were very interesting. The wind tunnel seemed to have many oblique shocks coming from imperfections and screws in the wind tunnel. This data may be used for future improvements to reduce these imperfections by discovering from where they emanate. An interesting discovery was difference of the test section Mach number from the pressure tap data and the inviscid one dimension area ratio. The actual pressure tap data showed a slightly lower Mach number than the inviscid theory. However, at the heart of the experiment were the differences from the one dimensional inviscid shock theory to the actual pressure tap data. A bottom surface boundary layer caused a separation of flow and forced the oblique shock forward of the ramp. The flow separated after the shock and then reattached. The flow then went through an expansion fan. Some very good oil flow visualization was taken to show these results. Schlieren System data also gave very good visualization of the actual shock location and angle to be used for comparison. Overall the smaller ramp angle seemed to agree more closely to the one dimensional theory.

Modern supersonic aircraft use high-performance low-bypass turbofan engines with afterburners to achieve supersonic flight as well as extreme maneuvering power. These engines require relatively smooth subsonic air in order to run properly and efficiently. In order to achieve this subsonic air the aircraft are required to generate shocks prior to the air entering the engine. This can be achieved by a normal shock at the engine nacelle inlet, though this has been found to be incredibly inefficient. Most supersonic aircraft use a series of oblique shocks that slow the supersonic air down gradually and with much less of a loss of energy from the flow. These oblique shock are created using “ramps,” or flat plates with varying angles to the flow. This lab explores oblique shocks off of a pair of similar ramps, one at 25 degrees and the other at 15 degrees in Mach 2.5 air flow. The shocks that these ramps create, as well as the flows that surround the shocks, can be studied to gain a better understanding of real high-speed flow.

The purpose of this experiment is to explore the properties of Mach 2.5 flow in a supersonic tunnel as it impinges upon a 15 degree or 25 degree ramp. This lab was performed in a 1.75 inch wide, Mach 2.5 tunnel. These experiments allow the graduate students involved to also gain valuable experience in studying high-speed flow with Schlieren images, pressure taps, and oil flow visualization.

Supersonic wind tunnels vary greatly in their construction, but they have components that make them alike. The airflow goes through a converging diverging nozzle like the one pictured below. The position with the smallest area is called the throat. When enough total pressure is located upstream, upstream conditions being region I, the flow is subsonic in region I and supersonic in region II. Region II is the test section area. Under the flow conditions of region I subsonic and region II super sonic the flow through the throat is sonic, or  $M = 1$ . This makes a convenient reference for measuring properties.

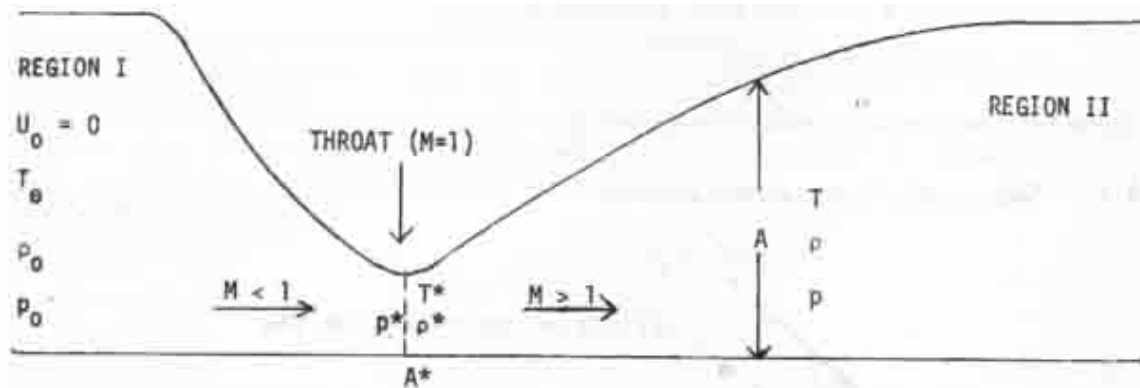


Figure 1 Supersonic Converging Diverging Nozzle

For the tunnel used in this experiment the throat area is fixed, which in turn means that the test section region II Mach Number is fixed.

The properties from the plenum, region I, are related to the test section properties by the following equations derived from the conservation of mass, momentum, and energy along with the perfect gas law. These equations are

$$\frac{P_o}{P} = \left(1 + \frac{\gamma - 1}{2} M^2\right)^{\frac{\gamma}{\gamma - 1}} \quad (1)$$

$$\frac{\rho_o}{\rho} = \left(1 + \frac{\gamma + 1}{2} M^2\right)^{\frac{1}{\gamma - 1}} \quad (2)$$

$$\frac{T_o}{T} = \left(1 + \frac{\gamma - 1}{2} M^2\right) \quad (3)$$

$$\left(\frac{A}{A^*}\right)^2 = \frac{1}{M^2} \left[ \frac{2}{\gamma + 1} \left(1 + \frac{\gamma - 1}{2} M^2\right) \right]^{\frac{\gamma + 1}{\gamma - 1}} \quad (4)$$

$$P = \rho RT$$

where  $p$  is the pressure at a point along the nozzle,  $\rho$  is the density,  $T$  is the temperature,  $M$  is the Mach number,  $A$  is the area, and  $\gamma$  is the ratio of specific heats. The “\*” denotes the sonic conditions at the throat and the “0” subscript indicates a total, or zero-velocity properties, from the plenum chamber. From these formulas and the plenum properties the flow conditions in the test section can be calculated.

Since the experiment deals with a supersonic test section some background information about supersonic shocks and expansion fans is needed. Shown below is a diagram of a supersonic flow around a sharp edged wedge. There is an oblique shock along with Prandtl-Meyer Expansion Fans.

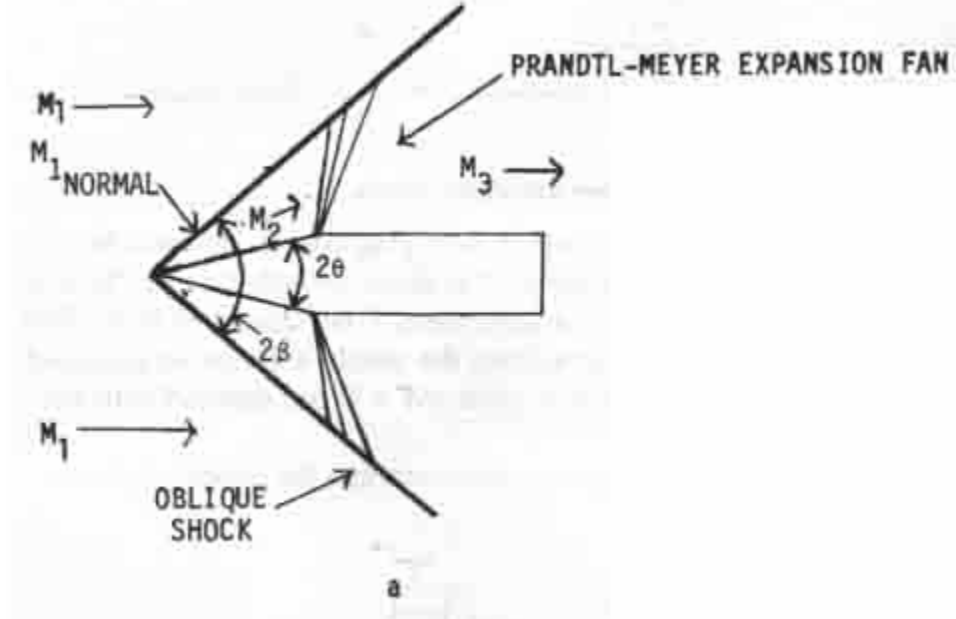


Figure 2 Supersonic Flow around Sharp Edged Body

The shock pictured is an oblique wave which starts at the edge. The relationship between the shock angle  $\beta$ , the wedge angle  $\theta$ , the Mach number ahead of the shock  $M_1$ , and the Mach number behind the shock  $M_2$  is found in the following two equations:

$$\cot(\theta) = \tan(\beta) \left[ \frac{6M_1^2}{5(M_1^2 \sin^2(\beta) - 1)} - 1 \right] \quad (5)$$

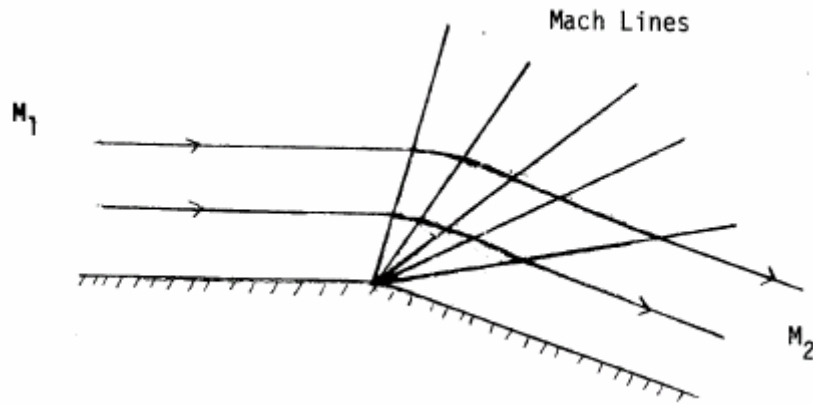
$$M_2^2 \sin^2(\beta - \theta) = \frac{1 + \frac{\gamma - 1}{2} M_1^2 \sin^2 \beta}{\gamma M_1^2 \sin^2 \beta - \frac{\gamma - 1}{2}} \quad (6)$$

The relation of total pressure,  $P_0$ , before and after the shock, can be found with the following equation:

$$\frac{P_{02}}{P_{01}} = \left[ \frac{6M_1^2 \sin^2(\beta)}{M_1^2 \sin^2(\beta) + 5} \right]^{\frac{7}{2}} \left[ \frac{6}{7M_1^2 \sin^2(\beta) - 1} \right]^{\frac{5}{2}} \quad (7)$$

The total pressure is the single most important piece of the puzzle to describe the flow following the shock, as the static pressure is dependant on this value. The static pressure comparison with the theoretical is critical to analyzing the supersonic ramp.

Once the shocks are taken care of the convex expansion waves must dealt with. These waves appear as in the figure below:



When the flow is turned in this manner the flow expands through a series of Mach lines. The simplified equation governing this expansion comes from the Prandtl Meyer functions:

$$v(M) = \sqrt{\frac{\gamma+1}{\gamma-1}} \tan^{-1} \sqrt{\frac{\gamma-1}{\gamma+1} (M^2 - 1)} - \tan^{-1} \sqrt{M^2 - 1} \quad (8)$$

where  $v(M)$  is the Prandtl Meyer function for the Mach number specified in front of or behind the expansion. The angle the flow is turned is defined as  $\Delta\theta$ . Then the values of flow turning angle and the two Prandtl Meyer functions before and after the expansion wave are related by the following function.

$$\Delta\theta = v(M_2) - v(M_1) \quad (9)$$

Now the computation of the shock flow field can be calculated.

A diagram of the supersonic wind tunnel used in this experiment is shown below.

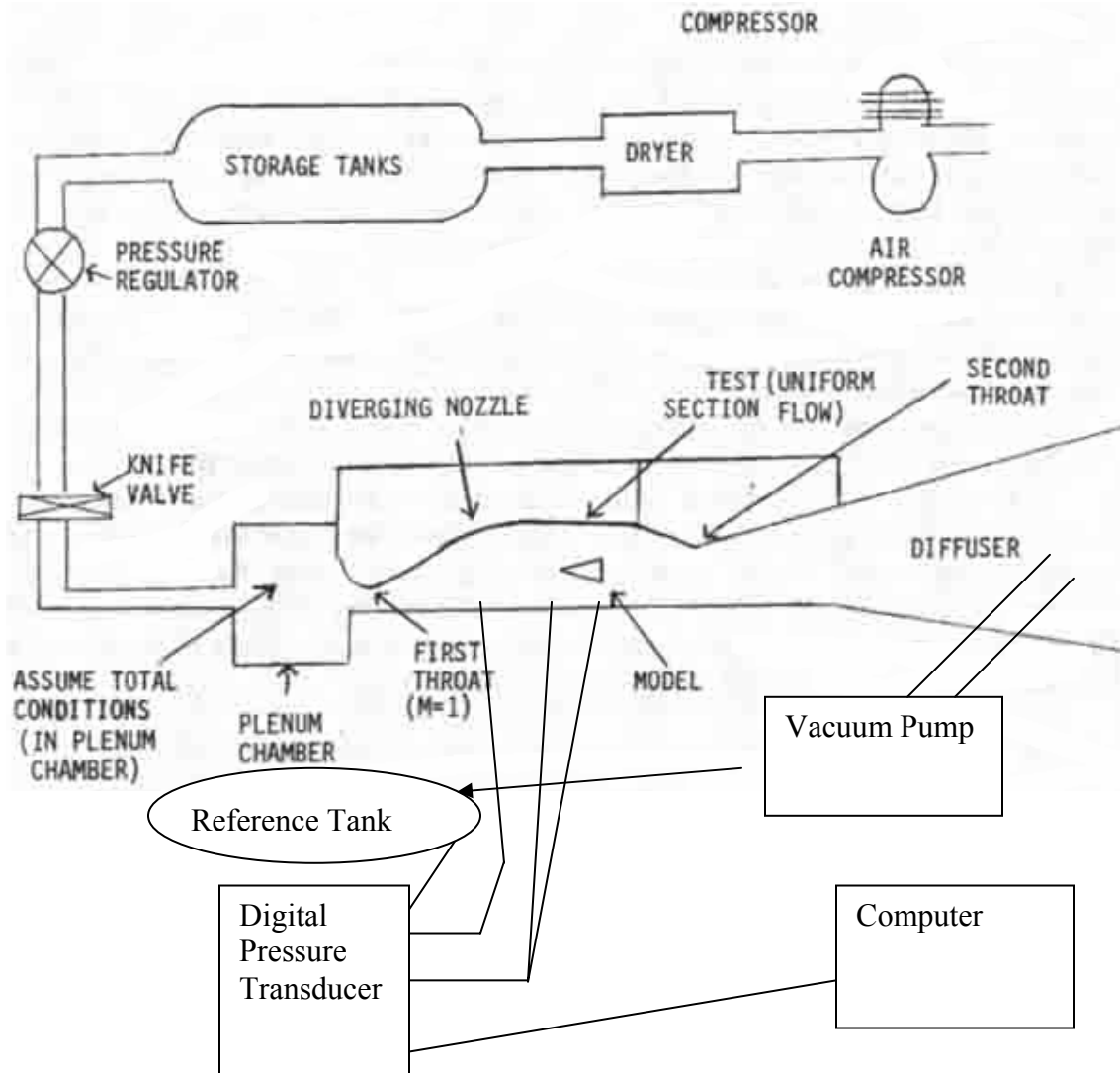


Figure 3 Schematic of Wind Tunnel

The air is first drawn through a compressor and dried. Then the air is stored in a 350 cubic feet storage tank. The air passes through the pressure regulator which allows the user to control the plenum pressure for the run. The knife valve is used as a quick way to open and close the airflow through the wing tunnel. This is necessary due to the large amount of airflow required to keep the flow supersonic. Then the flow passes into the plenum chamber where the flow turbulence is reduced and the total and static properties are assumed to be equal. This is due to the fact that the velocity is very small and assumed zero. The flow converges until it reaches the sonic conditions at the first throat. The flow then accelerates quickly until it reaches the test section, where the flow is at uniform velocity. The flow reaches the model and creates the shocks and expansion fans. The flow then goes through the second throat where the normal shock is created some distance after. The second throat decelerates the flow and keeps the normal shock out of the test section. After this a vacuum system pumps the total pressure down aft of the flow to reduce the total pressure further. This can also be turned off and set to atmospheric pressure. The vacuum tank also runs to a reference tank used for the digital

AAE 520L  
Lab Team 6  
3/15/2004

pressure transducer. The pressure transducer needs a vacuum reference to base the pressure taps from. The digital pressure transducer is also attached to several pressure taps varying along the nozzle and test body. The digital pressure transducer is also connected to a computer running pressure recording software.

Two separate systems are available for flow visualization. The Schlieren system and oil flow visualization. The Schlieren system is shown below for the wind tunnel.

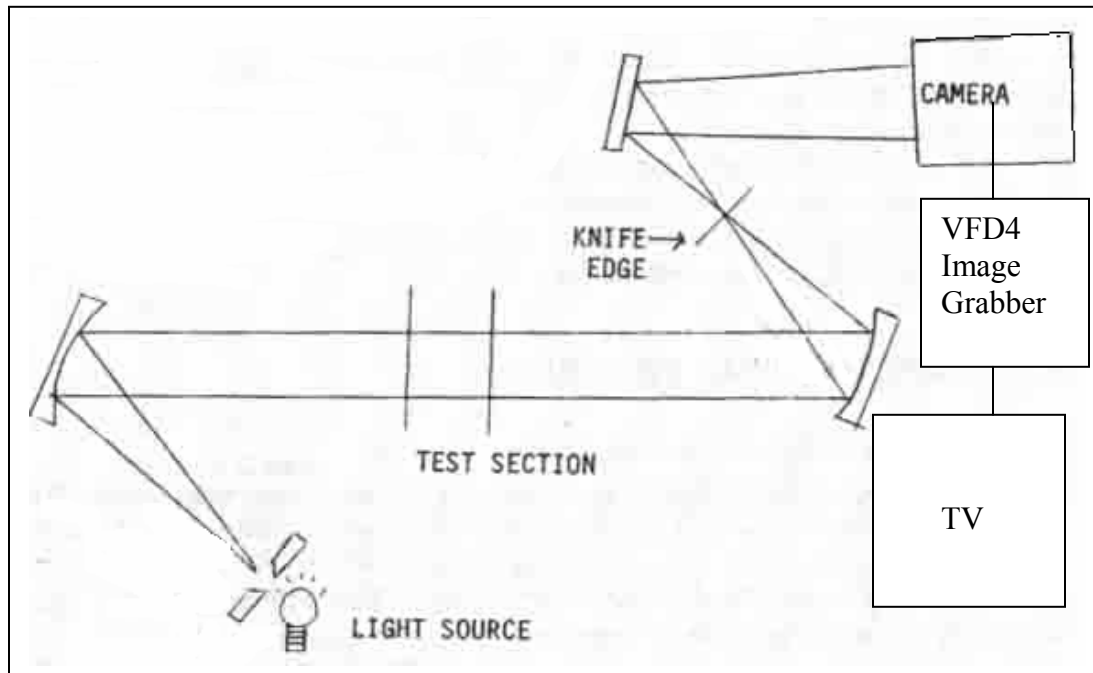


Figure 4 Schlieren System

The Schlieren system measures variations in density, which is very helpful in visualizing shock waves. The light source is filtered through a very small area and reflected off a mirror. The mirror passes through the wind tunnel and reflects off another mirror. This the image then passes through the knife edge, off another mirror and to the camera. The image can then be recorded on the VFD4 Image grabber system which is linked to a TV for viewing. The image is saved by pressing grab, and then Write on the device. The second method involves mixing oil and paint together and physically putting this mixture on the model. The paint then follows the flow once run through the wind tunnel. The paint then shows the flow patterns on the model.



**Procedure**

The lab procedure involved two ramp models being placed in a supersonic wind tunnel. The wind tunnel was run for a short period of time causing oblique shock waves and expansion waves to be formed on the flow field around the model. Pressure tap data on the model as well as the wind tunnel was taken. Flow visualization was conducted using a Schlieren System and oil painted on the model. A formal list of equipment used in the experiment follows. A sketch of the equipment can be seen in figure 3 *Schematic of Wind Tunnel* of the background section.

1. Supersonic Wind Tunnel
2. 15 degree and 25 degree pressure tapped ramp models.  
For pressure tap recording.
3. 15 degree and 25 degree pressure untapped ramp models  
For oil flow visualization.
4. Model Stand  
This holds the model in the correct place in the test section.
5. Air Compressor  
Builds up the necessary pressure to run the wind tunnel.
6. 350 cubic feet Air Tanks  
Stores the high pressure air after the compressor.
7. Mirrors  
Reflect the light source for the Schlieren System.
8. Projection Lamp  
Continuous light source for the Schlieren System.
9. Carriage  
Supports the Schlieren System and allows translation of the system.
10. CCD Camera  
Displays the shock waves from the Schlieren System on a TV.
11. VFD4 Image Grabber  
Records the picture from the CCD camera onto a floppy disk.
12. TV  
Displays the CCD camera image.
13. Heise Pressure Gauge  
Measures gage pressure in the plenum of the wind tunnel.
14. Digital Thermometer  
Measure the plenum temperature.
15. Plenum Chamber  
Acts to reduce the velocity close to zero from the pipes entering the wind tunnel, the plenum also damps out disturbances.
16. PSI 9010 Intelligent Pressure Scanner  
This measure the static pressure at 16 positions on the wind tunnel or test model. The pressures are recorded digitally to a computer.
17. Vacuum Vessel and Gauge  
This allows for a reference vacuum to be created. This is needed as a reference for the PSI Pressure Scanner.
18. Vacuum pump

This allows for the vacuum vessel to be pump to almost a vacuum, and also allows reducing the wind tunnel exhaust pressure below atmospheric.

19 Exhaust vacuum vessel

This tank allows reduced wind tunnel exit pressure runs.

20 Oil and white paint

For flow visualization.

21 Camera for taking pictures of flow visualization

The actual procedure for the experiment follows in three parts. These parts are preparing the tunnel and Schlieren System, running the experiments, and shutting down the tunnel.

The preparation of the tunnel started with opening up the air supply valves (Valve 1 and 3) to the wind tunnel. The pressure regulator was then turned on to control the pressure in the plenum chamber. The ambient temperature and pressure were recorded on a thermometer and barometer respectively. The vacuum pump was turned on and the valve connecting it the vacuum vessel was opened to create a vacuum in the vessel. The lab view pressure recording software was loaded on the computer and set to record. Next the Schlieren System was set up. The projection lamp was turned on along with the recording camera and VFD4 image grabber. This setup can be seen in figure 4 of the background section. The needle of the Schlieren System and the carriage were also calibrated to show a good image of the density differences as well as the test model on the TV. The Schlieren System was then ready to record.

The experiments were then run by first connecting the pressure tap hoses from the pressure scanner to the specified tunnel and model positions. The experiments were conducted in two separate days of experiments. The first days experiment consisted of pressure tap data and Schlieren data. In the first part the pressure tap hoses were connected only to the wind tunnel top surface to get a wind tunnel profile. The pressure taps connected are shown in the figure below marked in red circled. The pressure taps at location 5,6,and 7 were connected to the higher pressure capacity pressure taps on the pressure scanner.

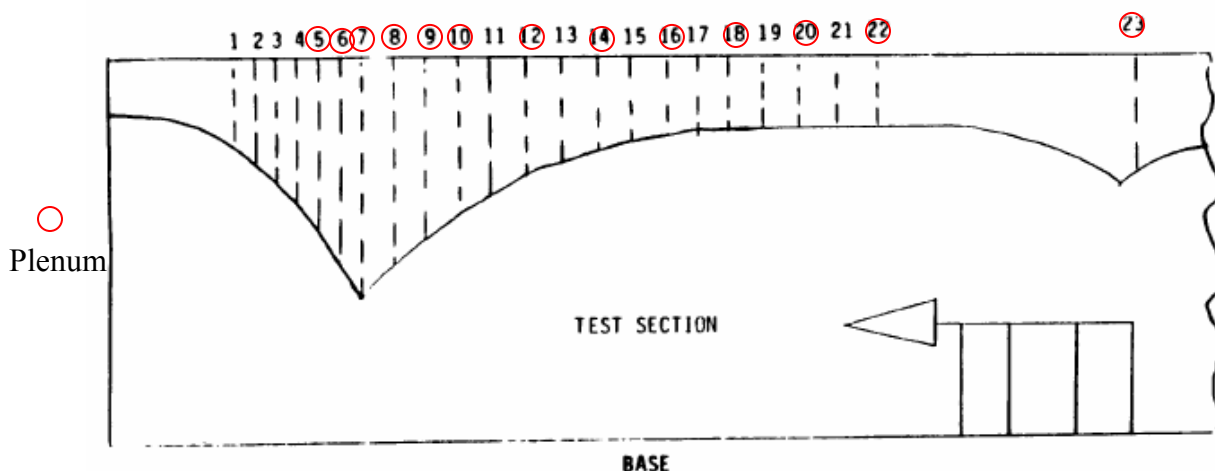


Figure 5 Pressure Taps Connected to Wind Tunnel

The pressure regulator was set to allow a gauge pressure of 43psi into the plenum. The vacuum vessel pressure was recorded and the pressure scanner was set to record on the computer. Next the wind tunnel needle valve was opened, starting the

wind tunnel. When the flow started the Heise gauge pressure and digital thermometer temperature were recorded. The needle valve was then closed, stopping the wind tunnel and the pressure scanner recording was stopped on the computer.

The second part was conducted with the pressure taps on the test model. The taps were relocated to positions on the test model seen below. The 25 degree ramp test body was inserted first.

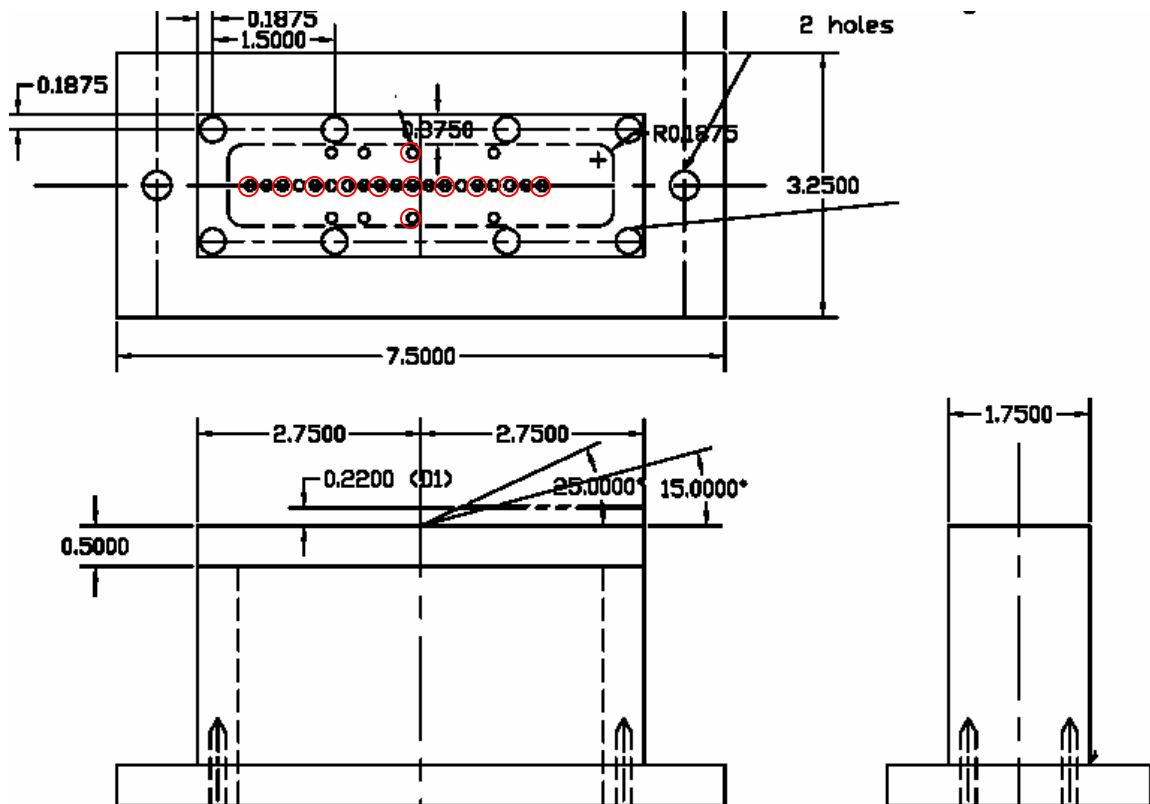


Figure 6 Test Models

The pressure regulator was set to allow a gauge pressure of 43psi into the plenum. The vacuum vessel pressure was recorded and the pressure scanner was set to record on the computer. Next the wind tunnel needle valve was opened, starting the wind tunnel. When the flow started the Heise gauge pressure and digital thermometer temperature were recorded. The GRB button on the VFD4 was pressed to record the Schlieren image. The needle valve was then closed, stopping the wind tunnel and the pressure scanner recording was stopped on the computer. The WR button was pressed next on the VFD4 to write the data to a disk, which was then transferred to the computer. This entire procedure was repeated for pressures of 43,56,58,60,59.5,61,56 gauge psi. Also three pressures were run with an exhaust vacuum set up to lower the exhaust pressure of the wind tunnel below atmospheric pressure. These were run at 60psi with a exhaust vacuum of 12inHG, 56psi and 20inHG, and 59.5psi and 9inHG. After this procedure was completed the 15 degree model was inserted in place of the 25 degree model and the whole

procedure was initiated again. This time the pressure regulator was set to give plenum gauge pressures of 61, 58, 60, and 61psi. The experiments for the second day consisted of taking pressure tap data only and no Schlieren pictures. The taps used for the pressure recording are shown below. These were used to get a better picture of the flow field near the separation point.

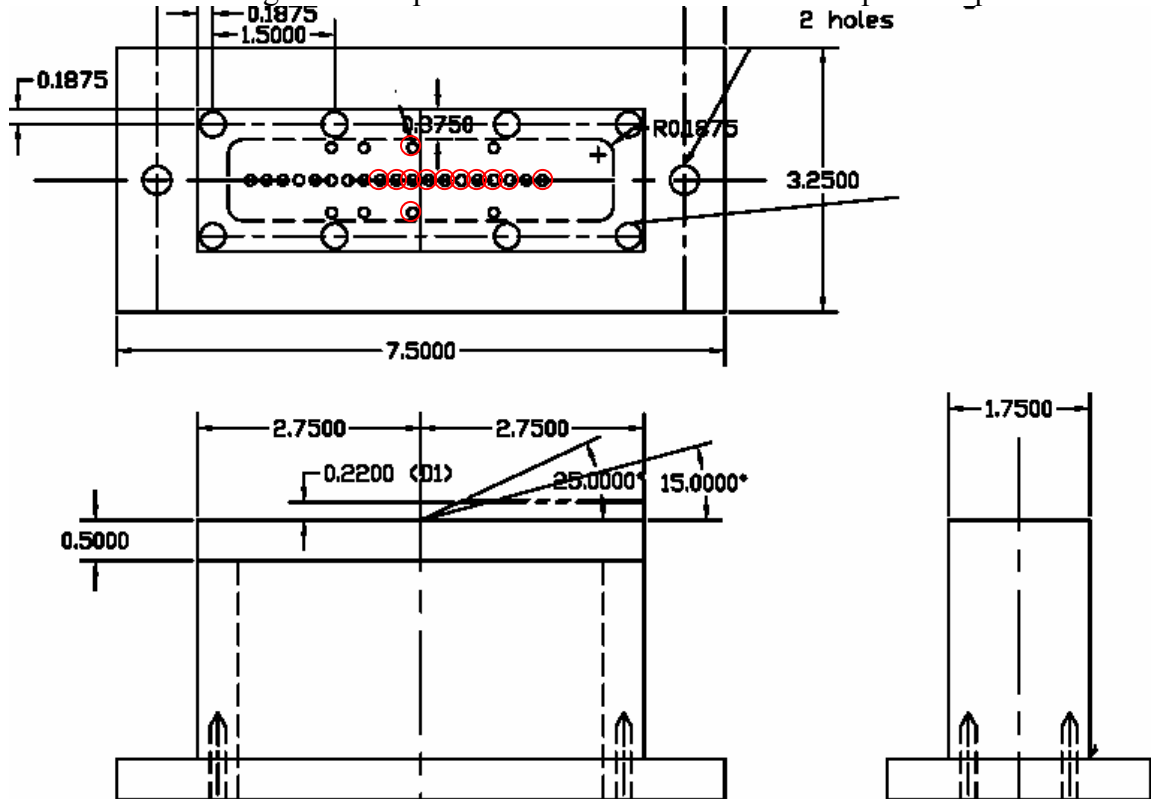


Figure 6 Test Models Day 2

The 15 degree test model was run at plenum gauge pressures of 60, 59.5, and 60psi. The 25 degree test model was run at plenum gauge pressures of 60, 57, and 56psi.

The next part of the experiment was flow visualization. The 25 degree test ramp was replaced with a model without pressure taps. A thin coat of oil was painted over the top surface of the model. Then many lines were painted across the model using an oil and paint mixture. The preparation can be seen in the picture below.



Oil Paint Preparation

AAE 520L

Lab Team 6

3/15/2004

The model was then placed in the wind tunnel and the wind tunnel was run at a plenum gauge pressure of 57. A picture was taken of each model through the wind tunnel window. Another picture of each model was taken out of the wind tunnel to see the flow lines. The model was then cleaned off and prepared again for the next run. Pressures of 60 and 61 psi were run next. Once this was accomplished the 25 degree ramp was taken out and the 15 degree ramp without pressure taps was inserted. Plenum gauge pressures of 50, 57, and 61 psi were run. Once again pictures of each were taken in and outside of the wind tunnel.

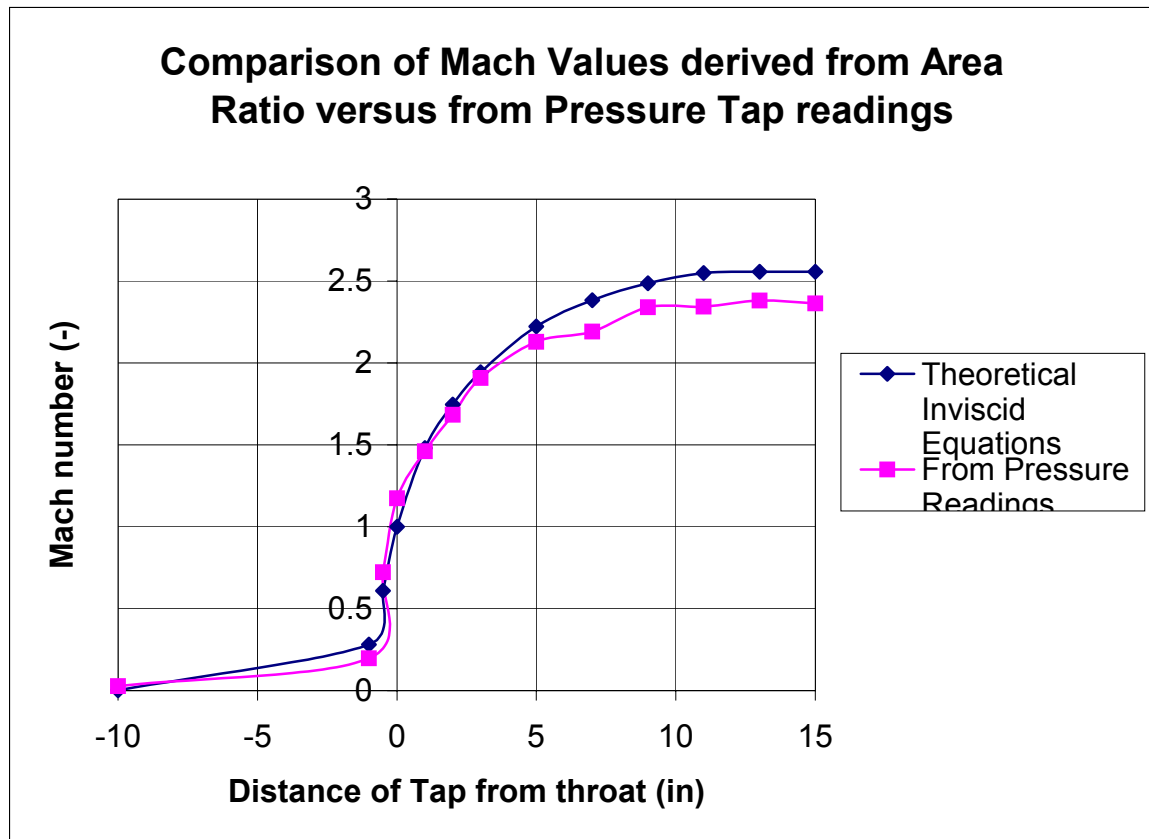
After these experiments the wind tunnel was shut down and all equipment was turned off. The pressure valves (1 and 3) were closed, and the pressure regulator was turned off. The needle valve was open to bleed all excess pressure out of the plenum.

## ***First Day***

### **No Model**

The first day of experimentation started with a test of the tunnel itself. The test team attached the pressure tap hoses from the pressure scanner to pressure taps along the top of the supersonic tunnel. Then a test was run to collect data on the Mach number within the tunnel and into the test section. This data was compared to the theoretical pressure readings calculated from the inviscid, 1-dimensional, flow equations (equations 1-4). These equations are hard to solve analytically and are thus usually referenced in table format. The lab team decided to use Microsoft Excel's iterative solver software to iterate the Mach numbers until the equations converged. This numerical solution technique adds some uncertainty and error, but it was decided to be much less than using tables and linear interpolation.

The Mach number comparison is shown below:



As can be observed from the chart, there is a small but significant difference between the theoretical and the actual Mach number. The test section, according to the

AAE 520L

Lab Team 6

3/15/2004

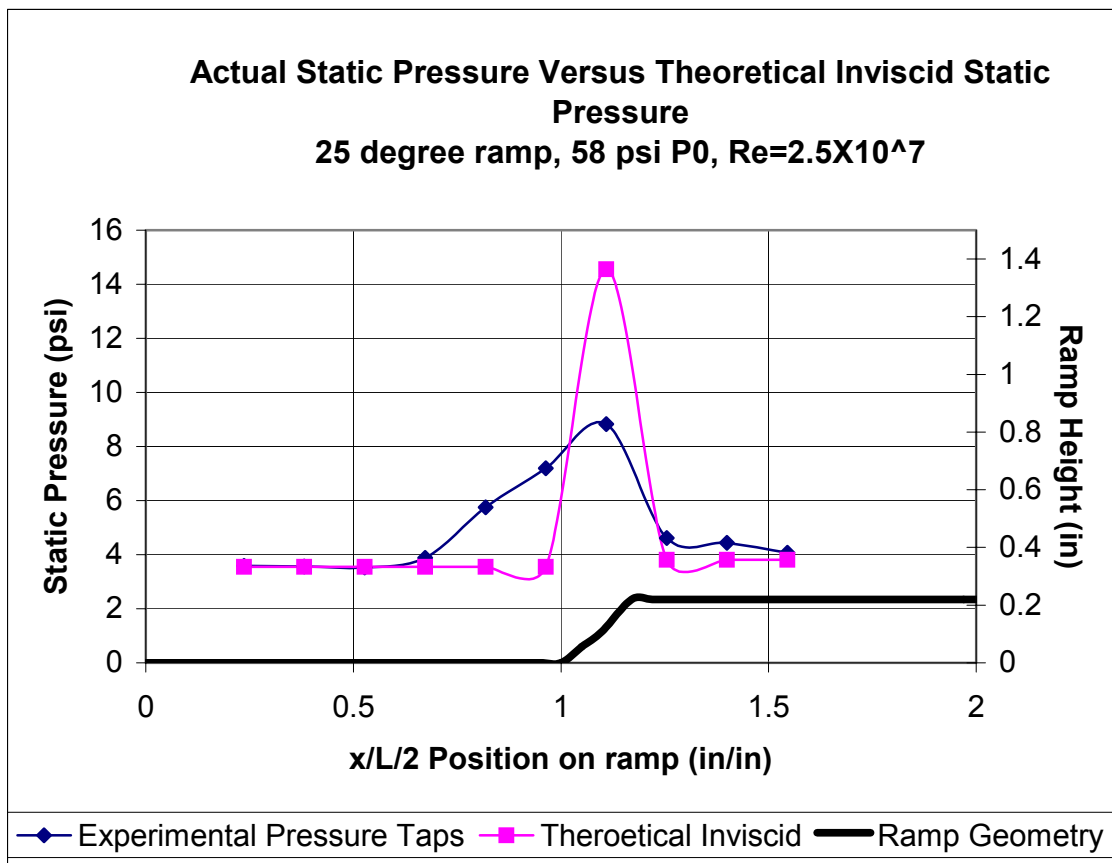
inviscid equations, should have a Mach number of approximately 2.56 or 2.6. According to the pressure tap readings, the actual Mach at the test section averages to 2.37. This difference in Mach number is most probably caused by a thick boundary layer formation, dirty walls in the tunnel and the many pressure taps ahead of the test section pressure taps. The boundary layer, as it gets thicker, will cause the effective area ratio of  $A/A^*$  in the test section to be much smaller than the physical walls of the tunnel. Any dirt or roughness on the sides of the tunnel, such as the pressure taps, may cause burbles in the flow or small shocks which will cause the pressure to increase along the sides of the tunnel and thus cause the tested Mach number to be less than expected.

During further experiments, the lab group found that the first few tap on the model itself seemed to be getting reliable pressure data. Of all the runs analyzed, the average Mach from the pressure readings on these taps was found to be about 2.46, or between 2.5 and 2.4. For each of the runs in which the forward taps on the model were available, an averaged Mach from each of the taps was used.

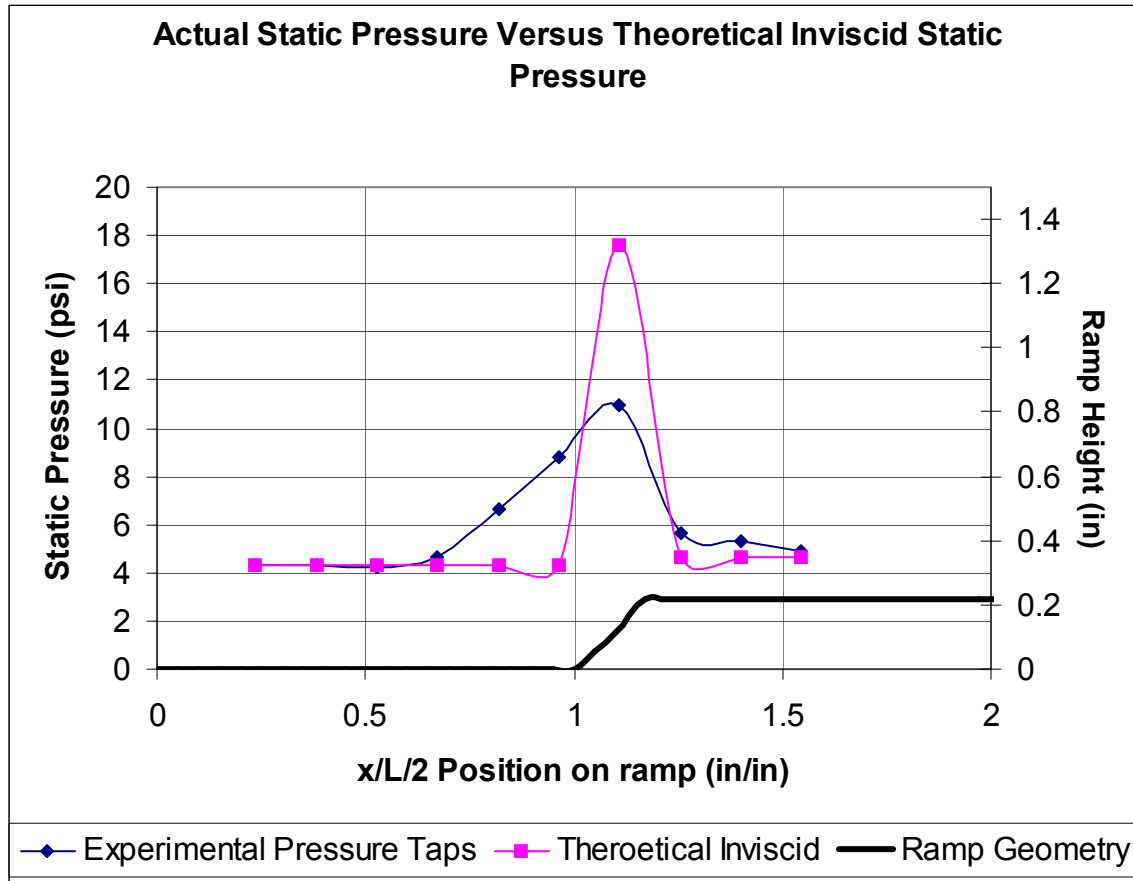
### 25-degree ramp experiment

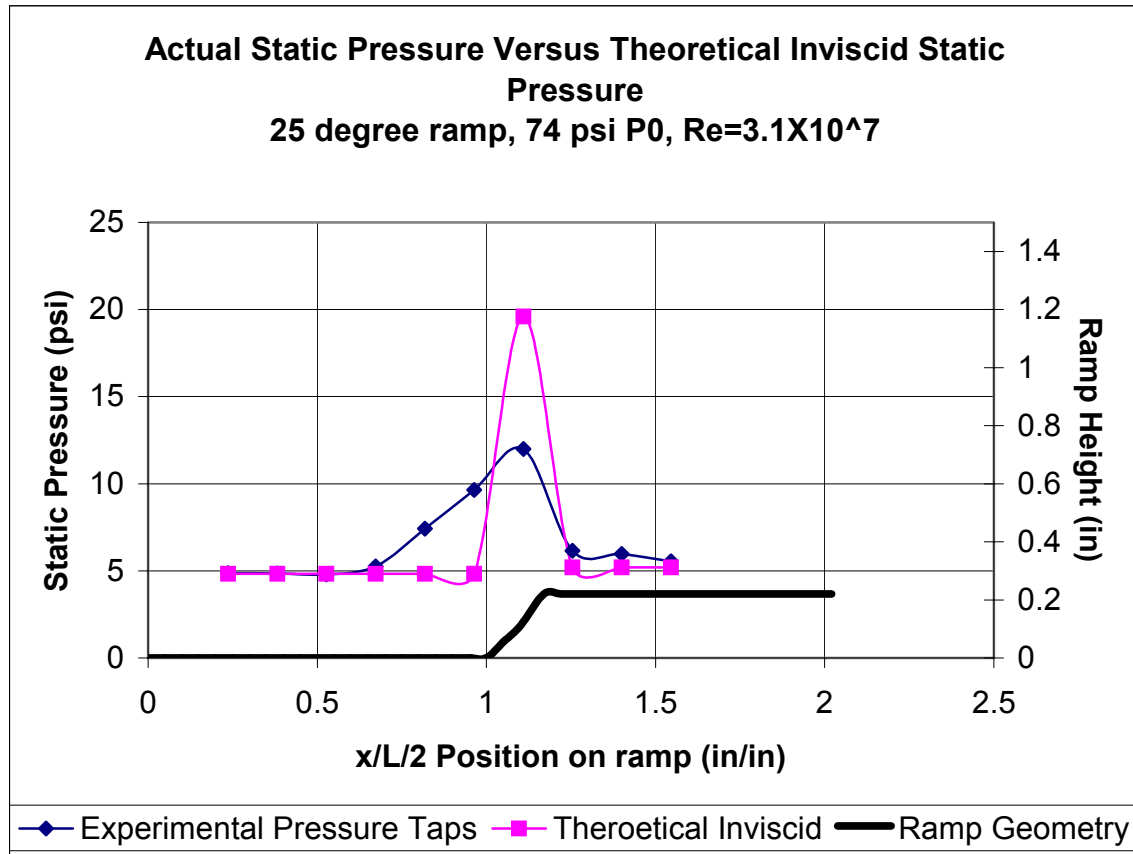
The 25-degree ramp model was then analyzed at plenum pressures of 58, 69 and 74 psi. absolute pressure. The Reynolds number was found using the static conditions at the beginning of the ramp angle and the characteristic length from the throat to the beginning of the ramp angle. The Mach number for the run was found by averaging the pressure reading of the first three pressure taps, and iteratively solving for the Mach number. The theoretical pressure readings came from using the Mach number for the run and then using equation 1 to find the pressure ratio to the plenum pressure. The theoretical Mach and oblique shock angles were found by iterating equations 5 and 6. The total pressure was found with equation 7, which was then used with the new Mach number and equation 1 to find the static pressure on the ramps. The expansion Mach was found from the iteration of equations 8 and 9, and then equation 1 was used again to find the static pressure on the model.

The comparison of the actual static pressure readings and the theoretical inviscid static pressure readings are shown below in the following three graphs:



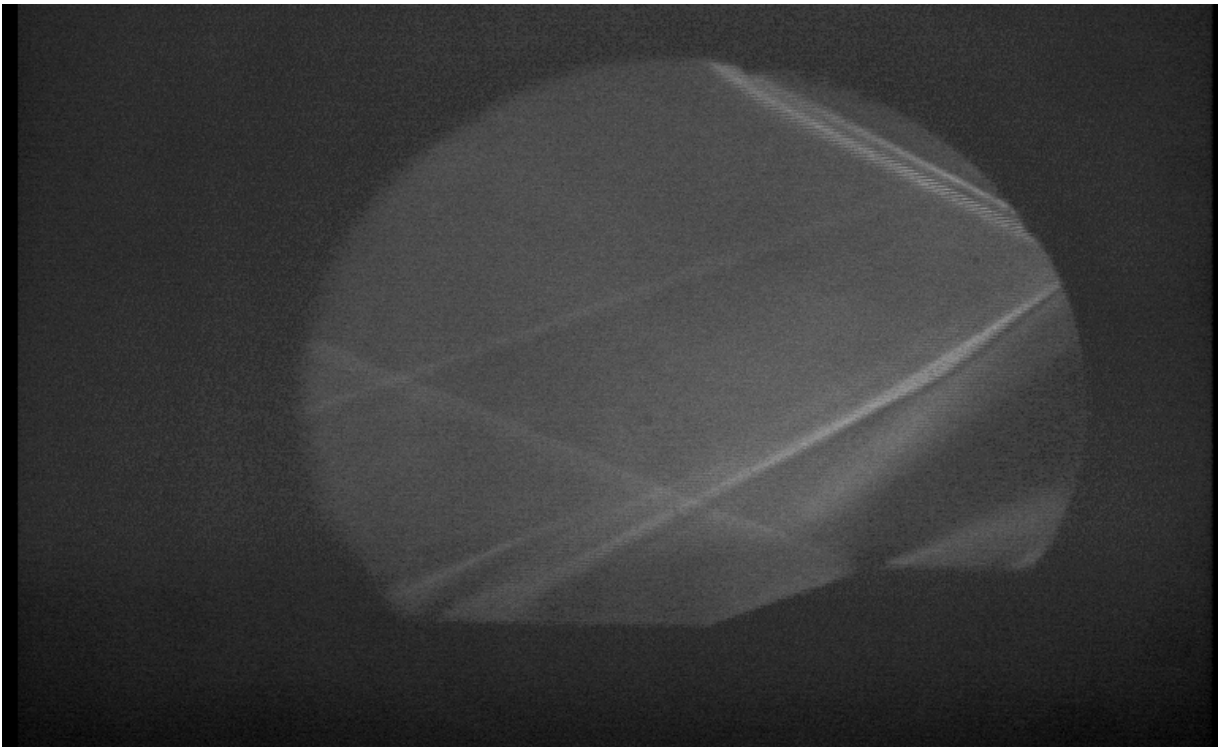
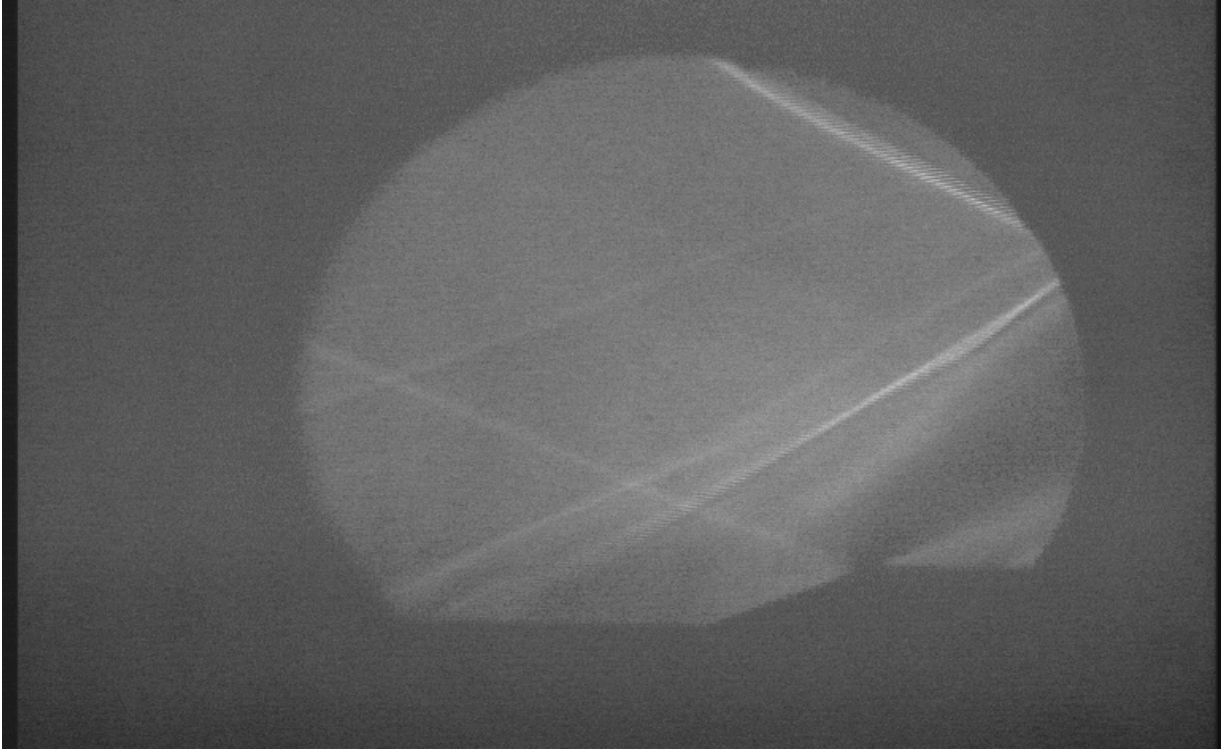




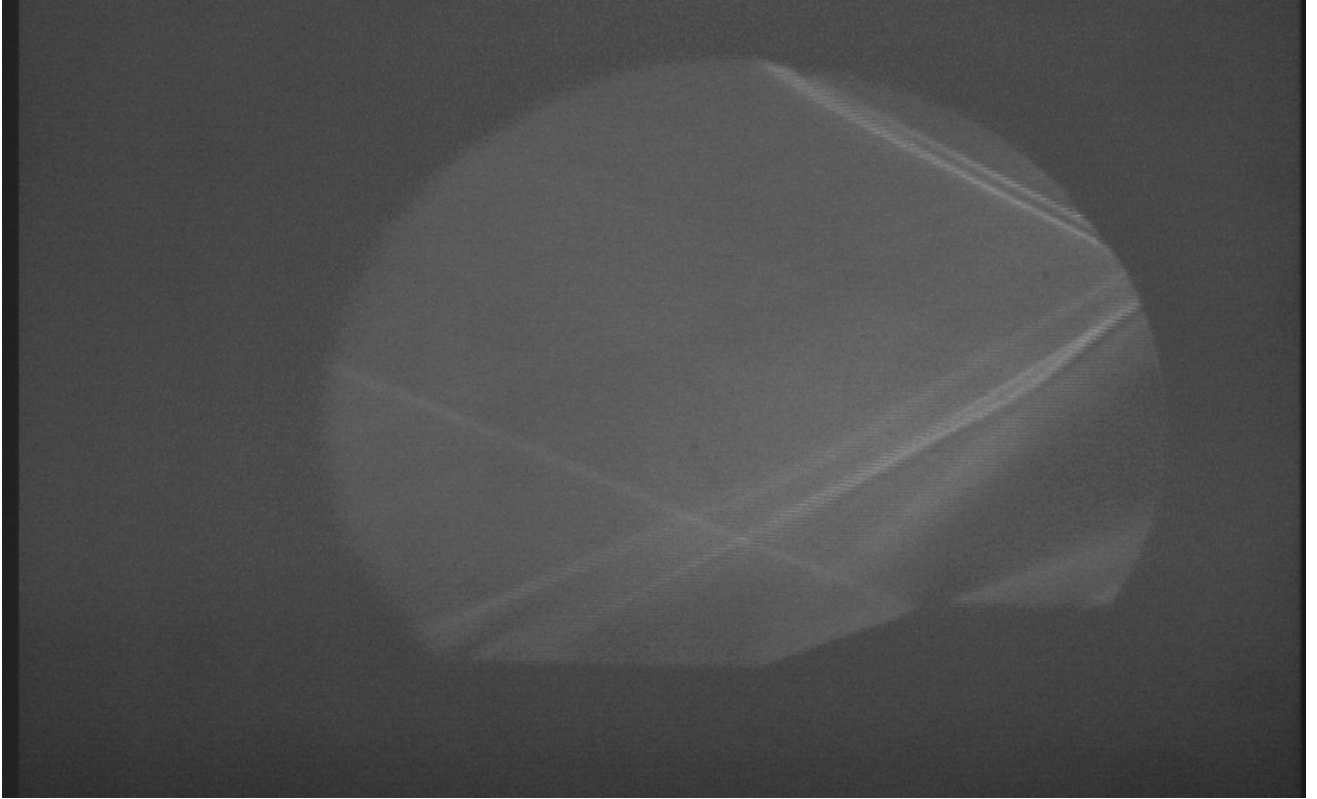


As can be seen in the graphs above, there is a significant difference between the theoretical and the actual static pressures across the shock. This is most certainly caused by viscous flow effects. It is important to note the pressure rise significantly ahead of the theoretical shock, this can be answered by the following three Schlieren images for the 58 psi, 69 psi, and 74 psi case respectively:

AAE 520L  
Lab Team 6  
3/15/2004

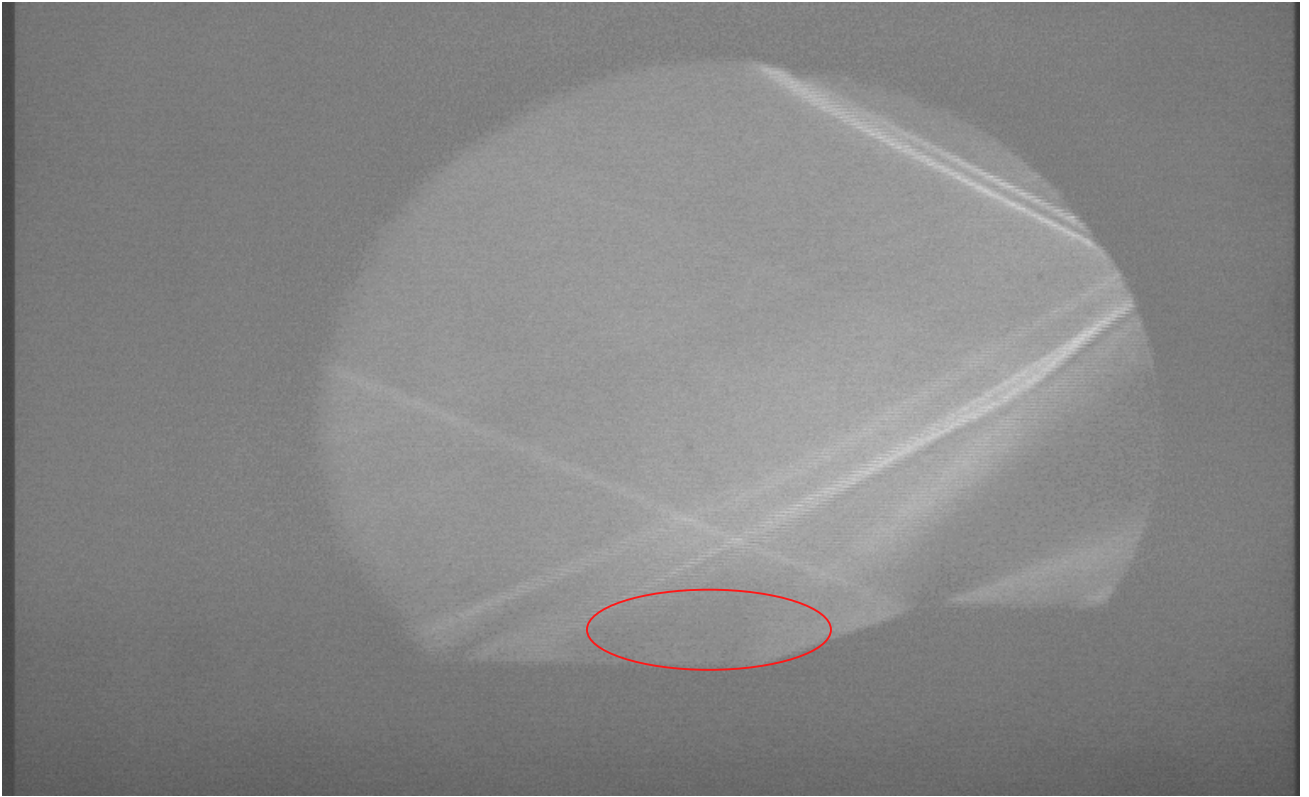


AAE 520L  
Lab Team 6  
3/15/2004

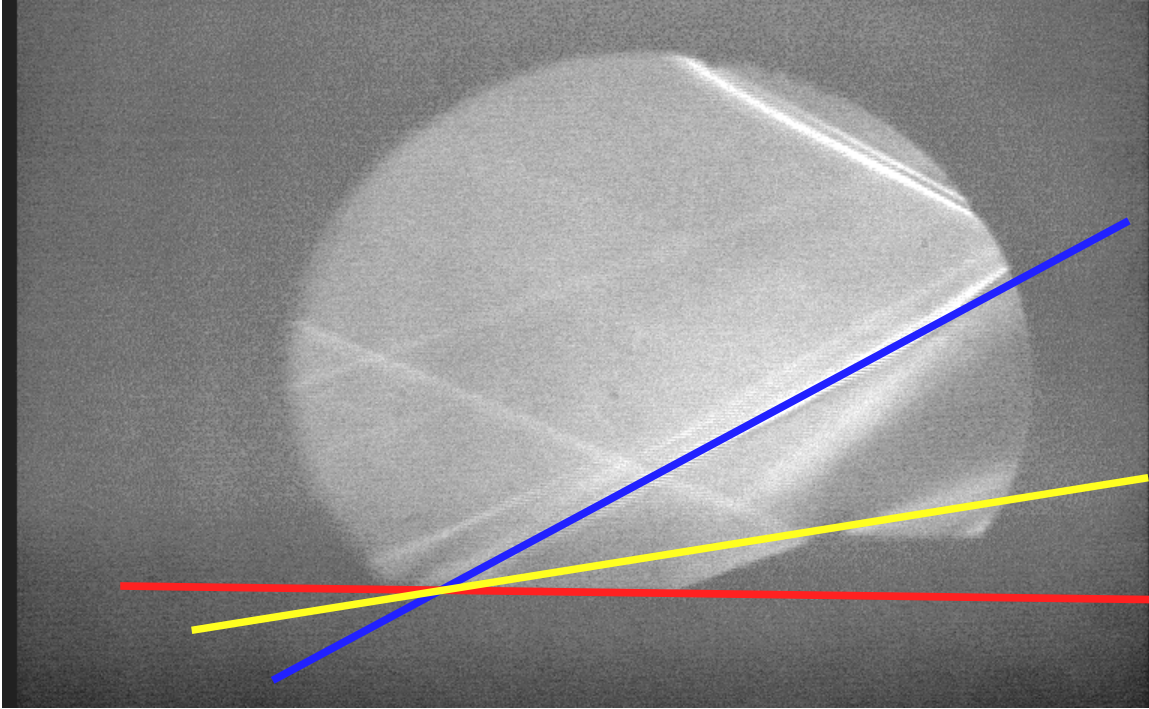


As can be see from these schlieren images, there is a shock well ahead of the ramp. There is also a separation bubble shown more visibly below:

AAE 520L  
Lab Team 6  
3/15/2004

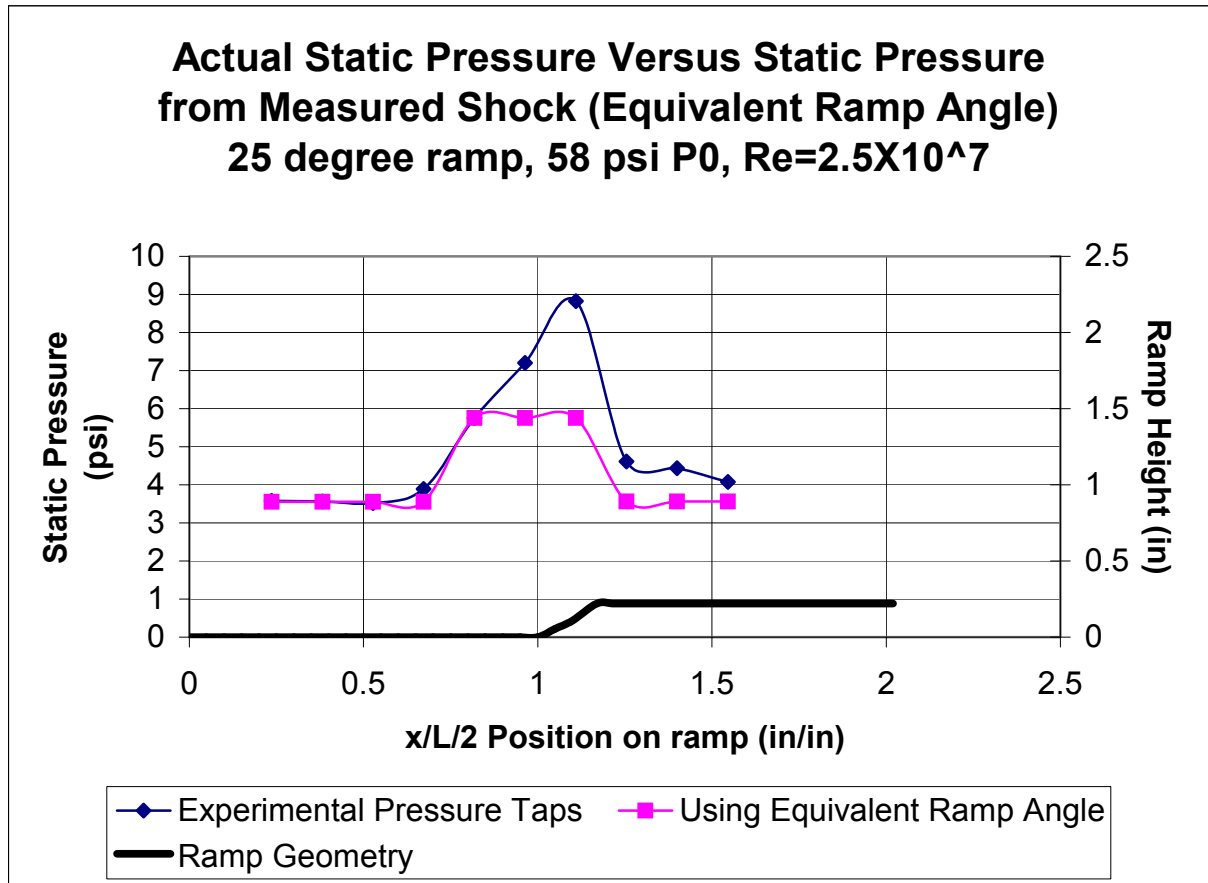


It was decided to see if there was a better way to predict the pressure readings through the shock. The lab team used lines drawn on the Schlieren images, for emphasis, to measure the angles of the shock and of what the effective ramp angle might be. An example of one of these images is shown below:

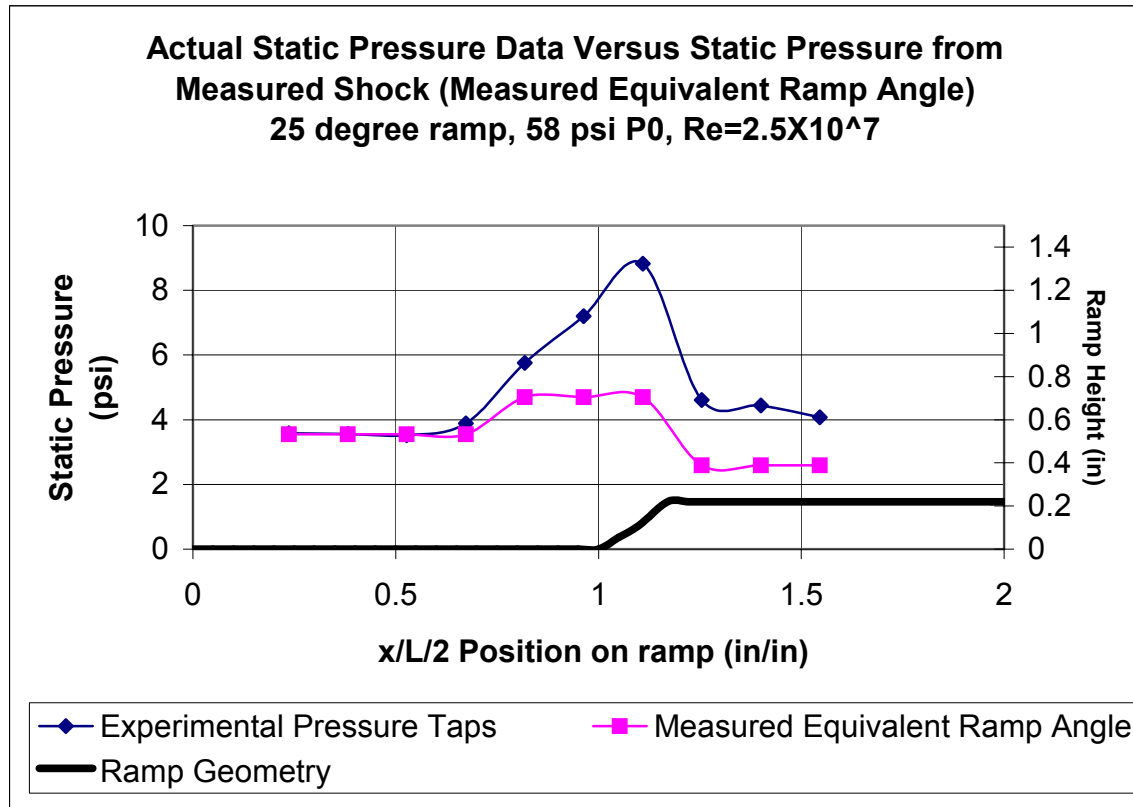


The shock angle (blue line) was found to be 30-degrees and the measured effective ramp angle was found to be 9 degrees. The 30-degrees is an especially large change from the theoretical 50-degree shock that was predicted. This could cause serious errors in performance of a system that was depending on the 50-degree shock wave.

The first comparison that was analyzed used the measured shock angle and known Mach number in equation 5 to find the calculated effective ramp angle. The ramp angle was then used for the pressure readings and expansion fan computation to produce the following comparison:

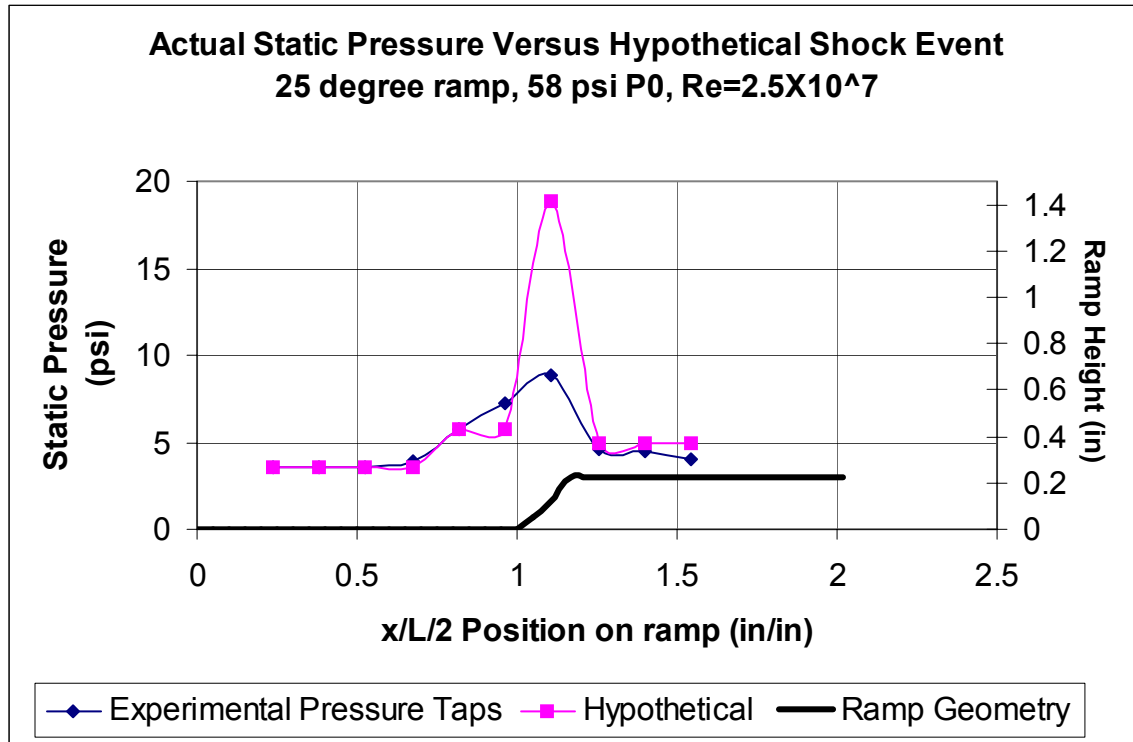


This comparison was only good through the initial shock. The next comparison is using the measured effective ramp angle. This comparison is shown below:



This was the worst prediction of them all, with very few points matching after the shock. The final comparison was done with a hypothetical model, wherein the lab group predicted that there were multiple shocks that occurred through the ramp, followed by the expansion fan. The model used the calculated equivalent ramp followed by the total pressure being lowered to that of the theoretical model at the end of the ramp, and then followed the expansion fan that was theoretically predicted. This comparison is shown below:

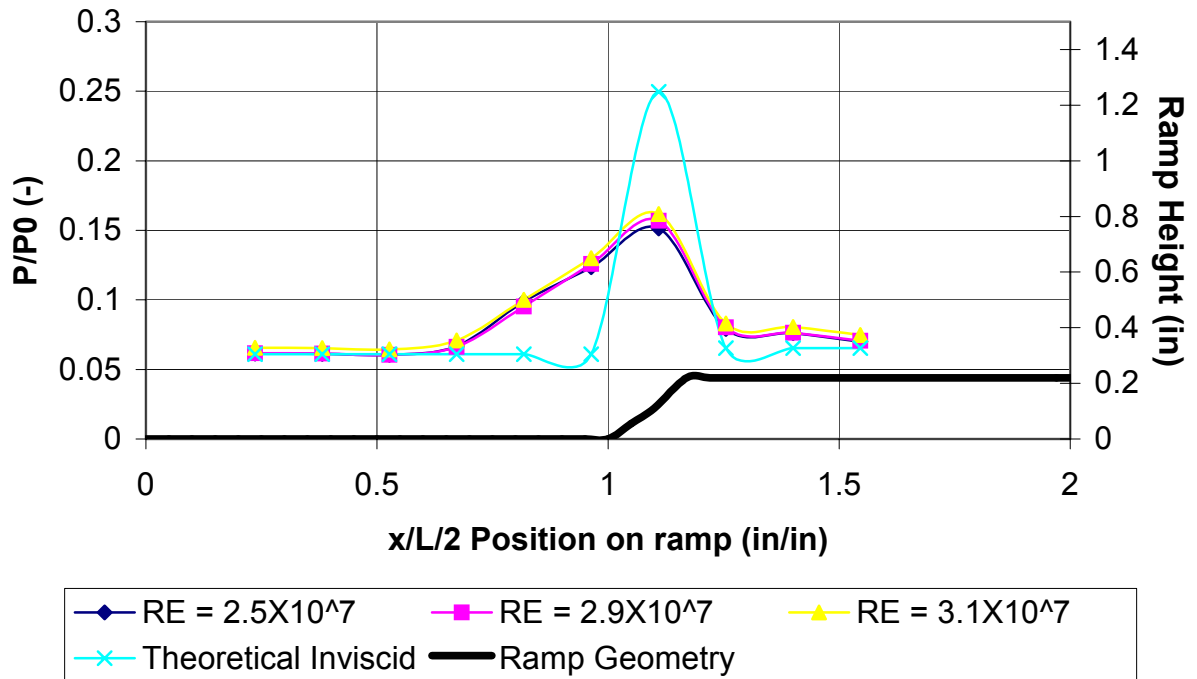




As can be seen, this model is not very accurate, but it shows a little promise as that maybe with more data, a set of shocks imitating the viscous flow can be made. The theoretical inviscid flow equations used originally seemed to be the best, though they are a poor model directly in the shock area and the separation bubble ahead of the ramp.

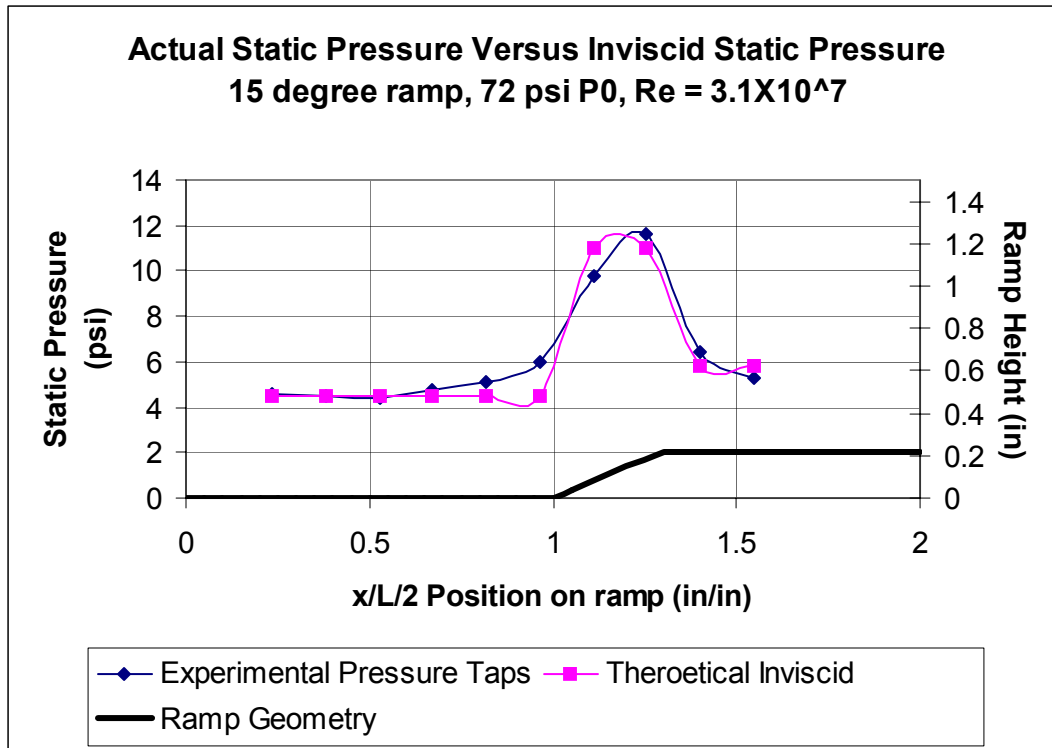
As a final comparison, the ratios of the static pressures to the plenum pressures are mapped below for each of the Reynolds number runs. Simultaneously they are being compared to the theoretical pressure ratio.

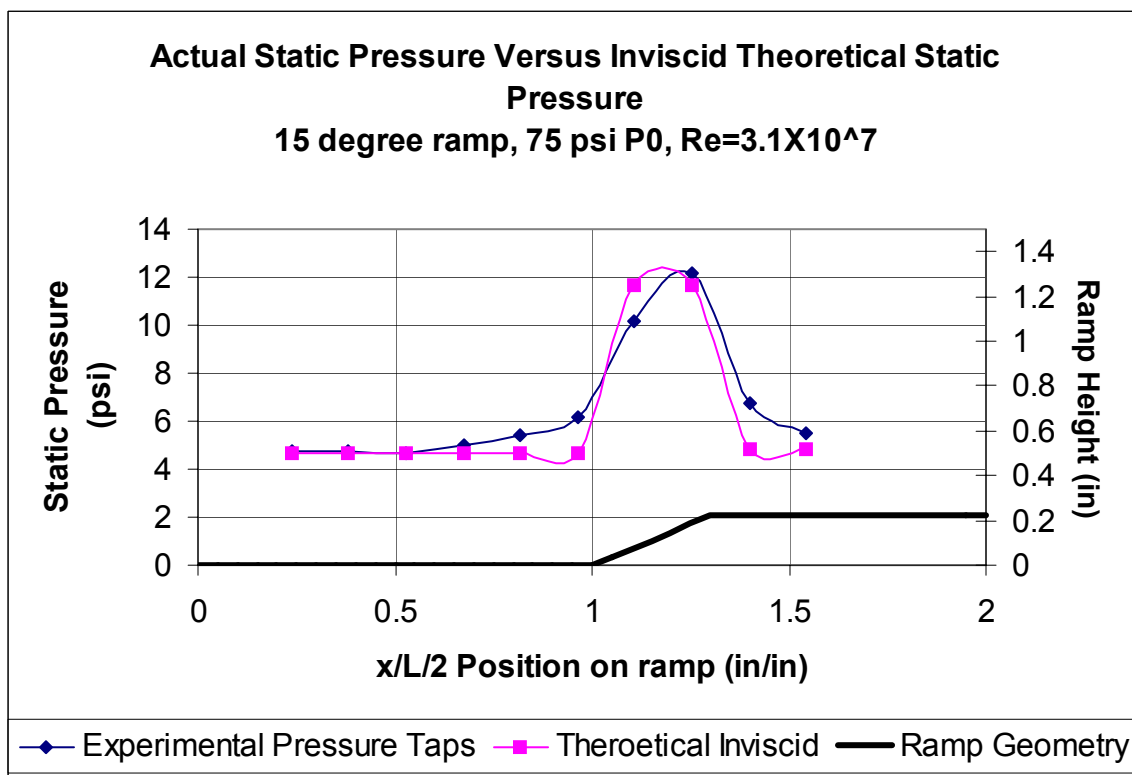
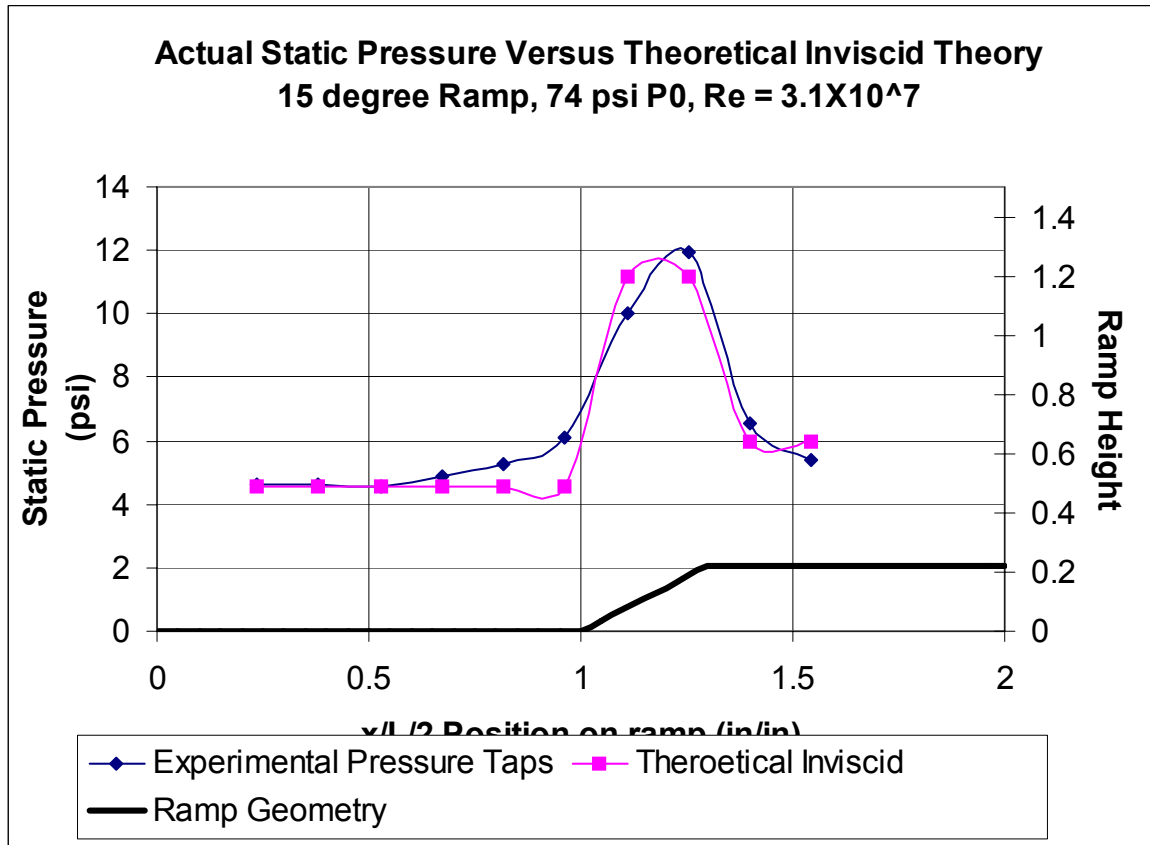
### Actual Static Pressure Comparison of Varying Reynolds Number with Theoretical Inviscid Static Pressure (25 degree ramp)



### 15-degree ramp experiment

The 15-degree ramp experiment was analyzed in the same manner as the 25-degree ramp. The first comparisons shown are the static pressures versus theoretical inviscid static pressures for 72 psi, 74 psi, and 75 psi plenum pressures respectively in the 3 following figures:

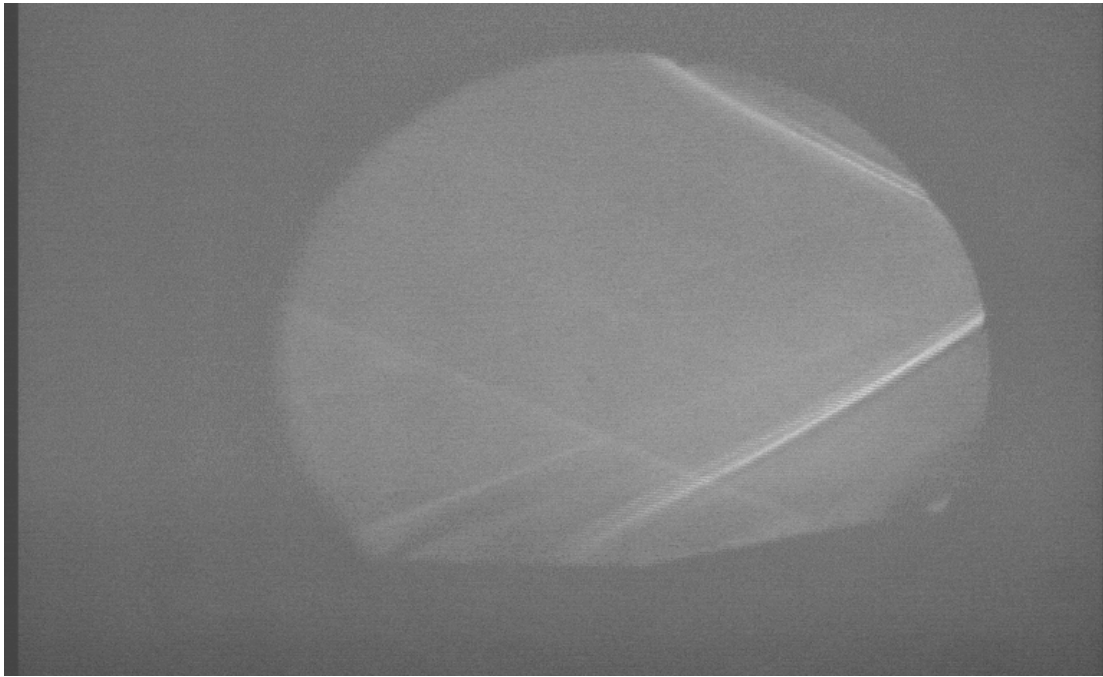




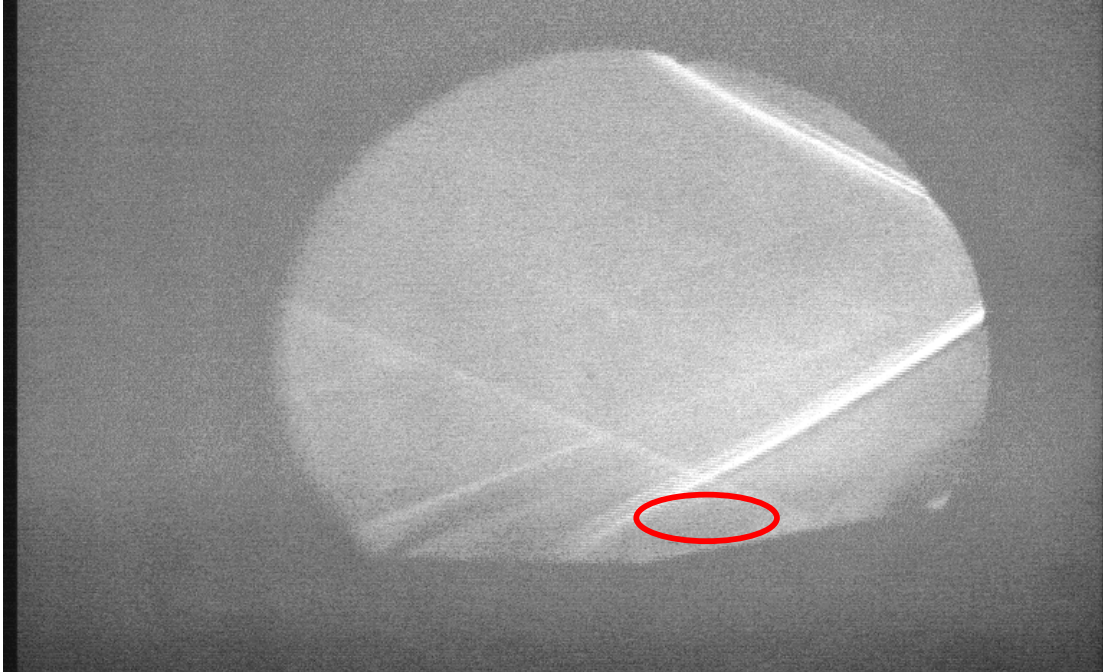
AAE 520L  
Lab Team 6  
3/15/2004

As can be seen from these three plots, the 15 degree ramp compares much more favorably with the theoretical behavior than the 25 degree ramp. This is rather intuitive as a sharper angle would logically seem to cause greater disruption in the flow.

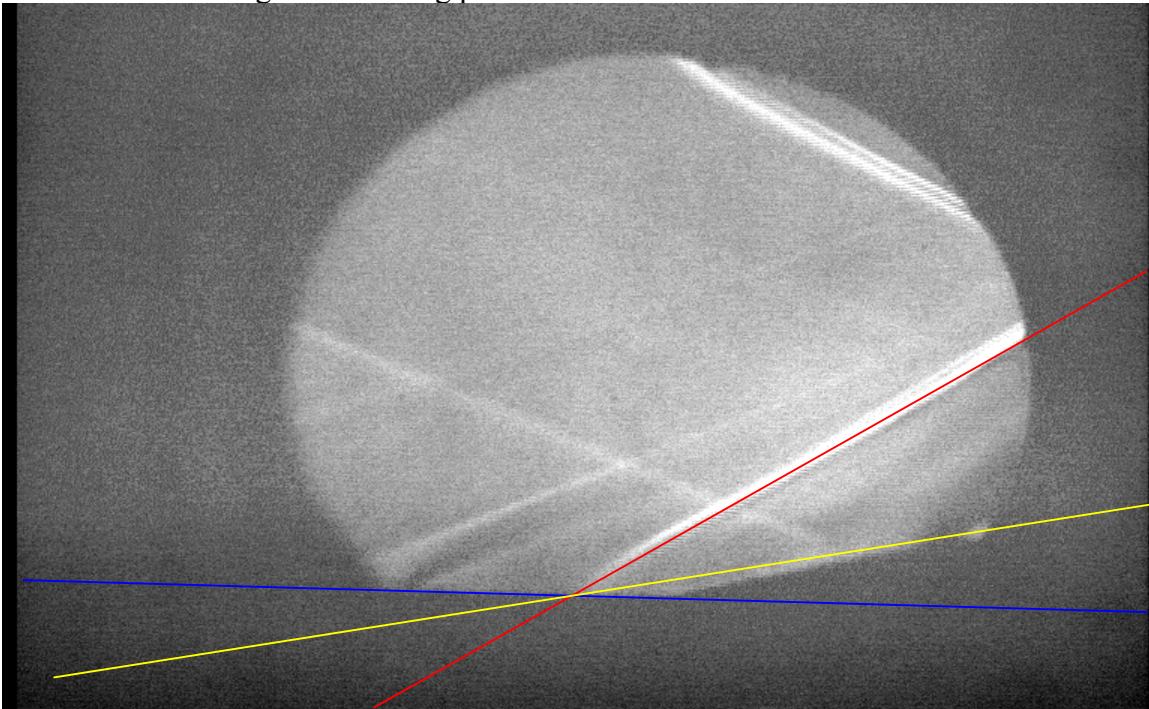
The Schlieren pictures still reveal much amiss with the actual versus theoretical as the following picture shows:



The shock is now much closer to the ramp, but still not quite there. There is still a separation bubble as shown below:



As before with the 25-degree ramp, the shock angle and effective ramp angle were measured using the following picture:

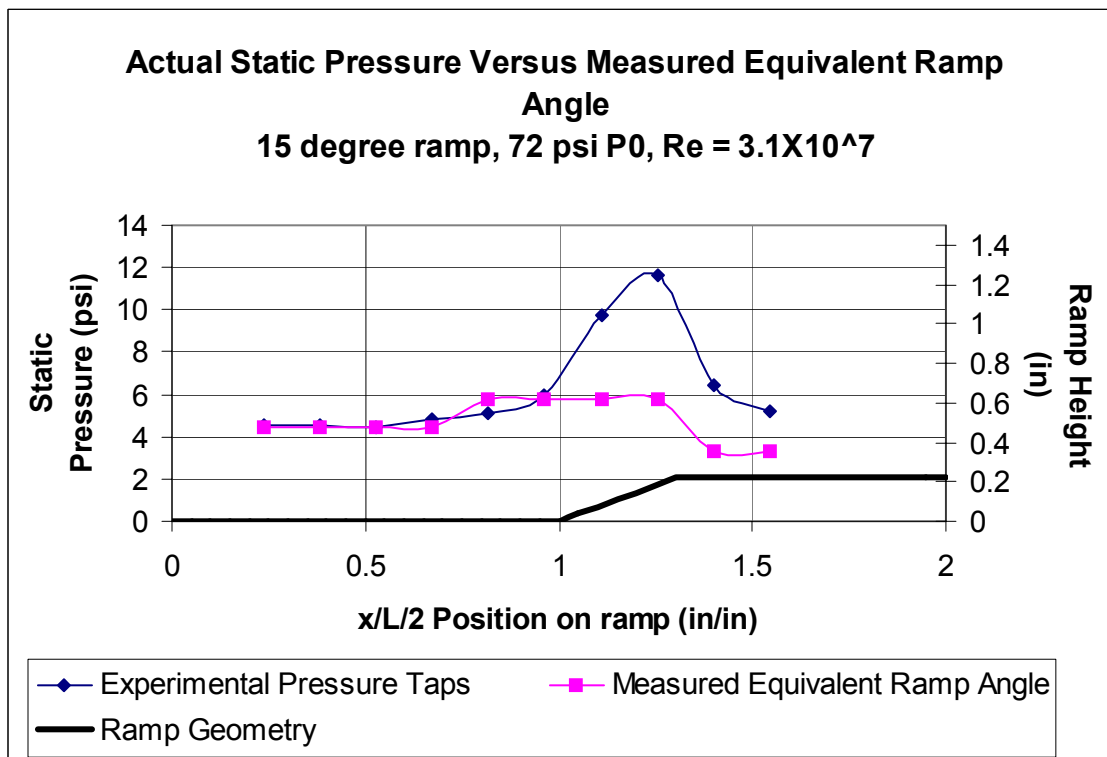
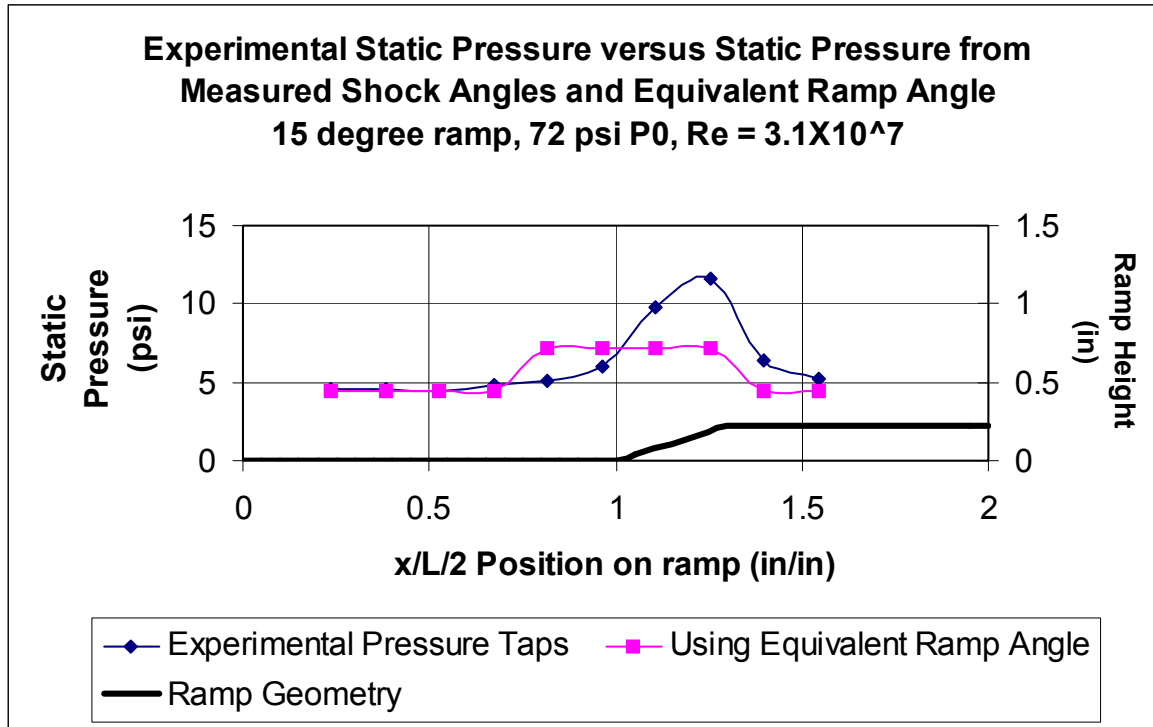


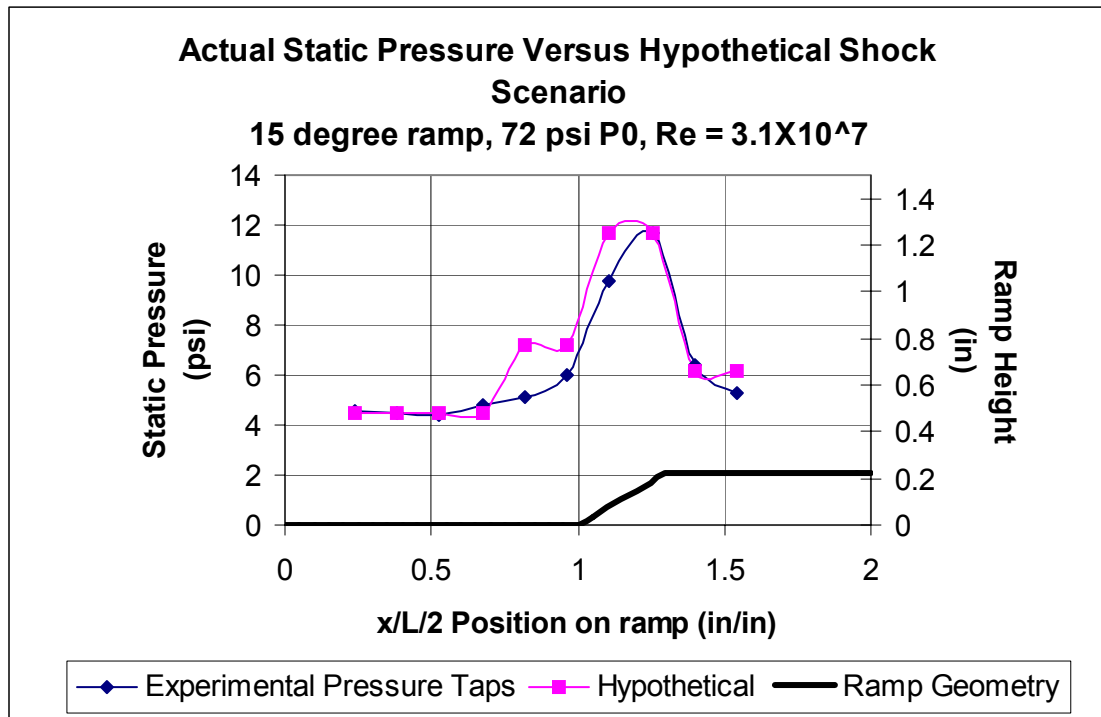
The shock angle was found to be 30 degrees (red line) and the measured effective ramp angle was found to be 9 degrees (yellow line). The theoretical shock angle was supposed to be 37 degrees. These are actually quite close.

As with the 25-degree ramp, the lab group attempted to find a better model of the shock and expansion. The first graph uses the calculated equivalent ramp angle and the

AAE 520L  
Lab Team 6  
3/15/2004

actual shock angle to find the static pressures, while the second graph uses the measured effective ramp angle to find the static pressure measurements, and the third graph uses the hypothetical shock interaction to predict the static pressure values.



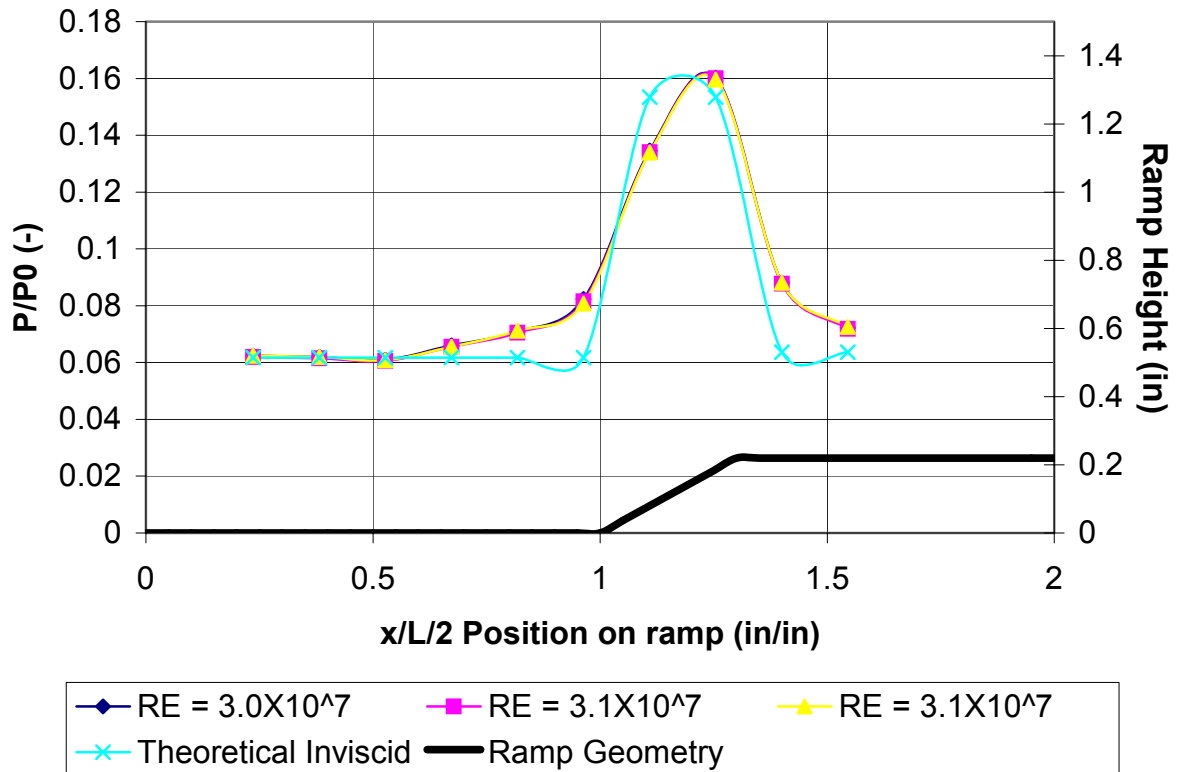


Again it appears as though the theoretical is the best, if not perfect, predictor of what happens after the ramp. The Hypothetical model got very close, but was not very good at the initial shock effects, and also there appears to be more pressure predicted after the expansion fan than actually was detected.

The final comparison is between the three different Reynolds number and the theoretical model. As with the 15 degree model this compares the pressure ratios ( $P_{\text{static}}/P_{\text{total}}$ ) for each of the experiments and the theoretical ratios.



### Actual Static Pressure Comparison of Varying Reynolds Number with Theoretical Inviscid Static Pressure (15 degree ramp)



AAE 520L

Lab Team 6

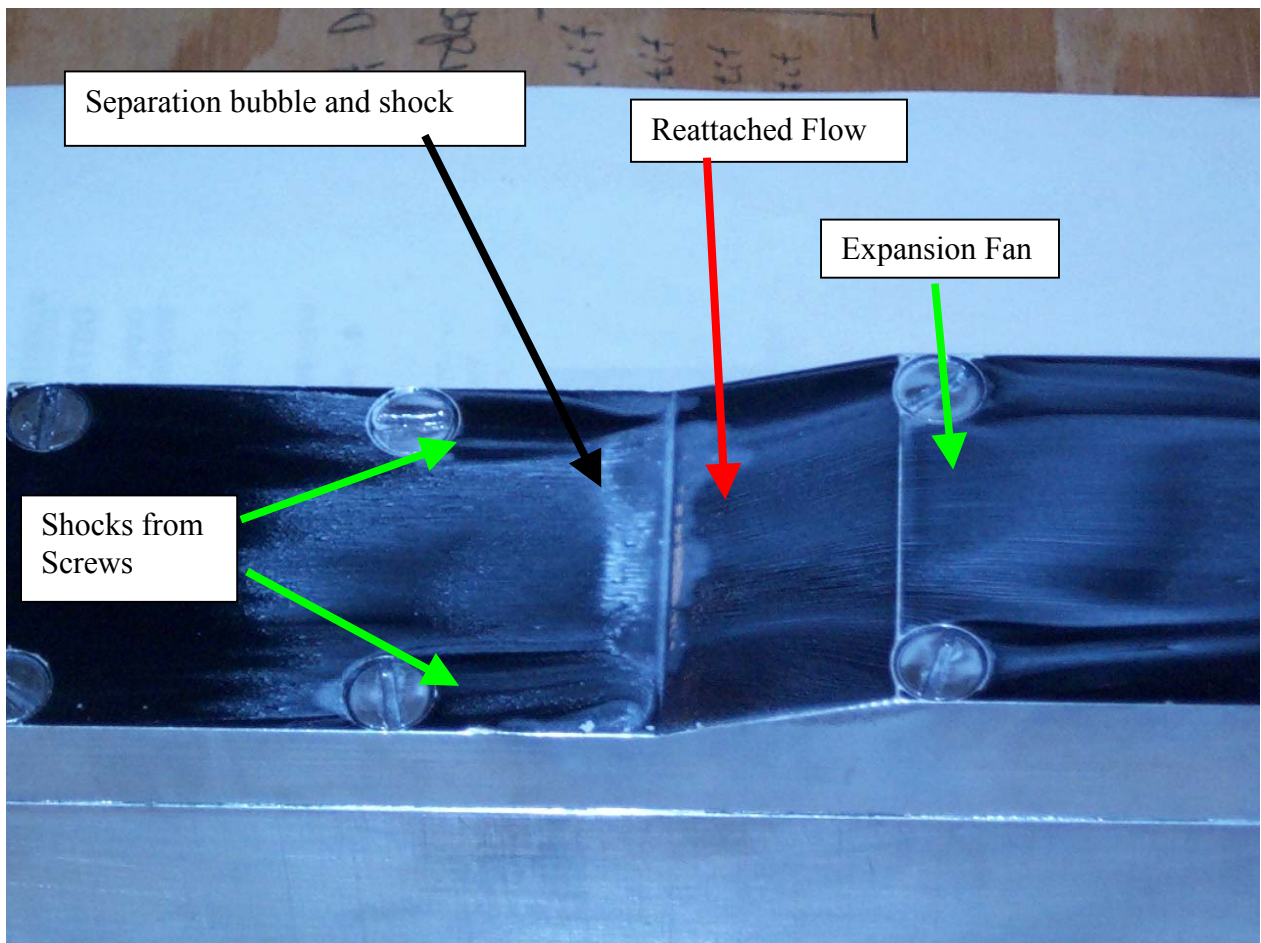
3/15/2004

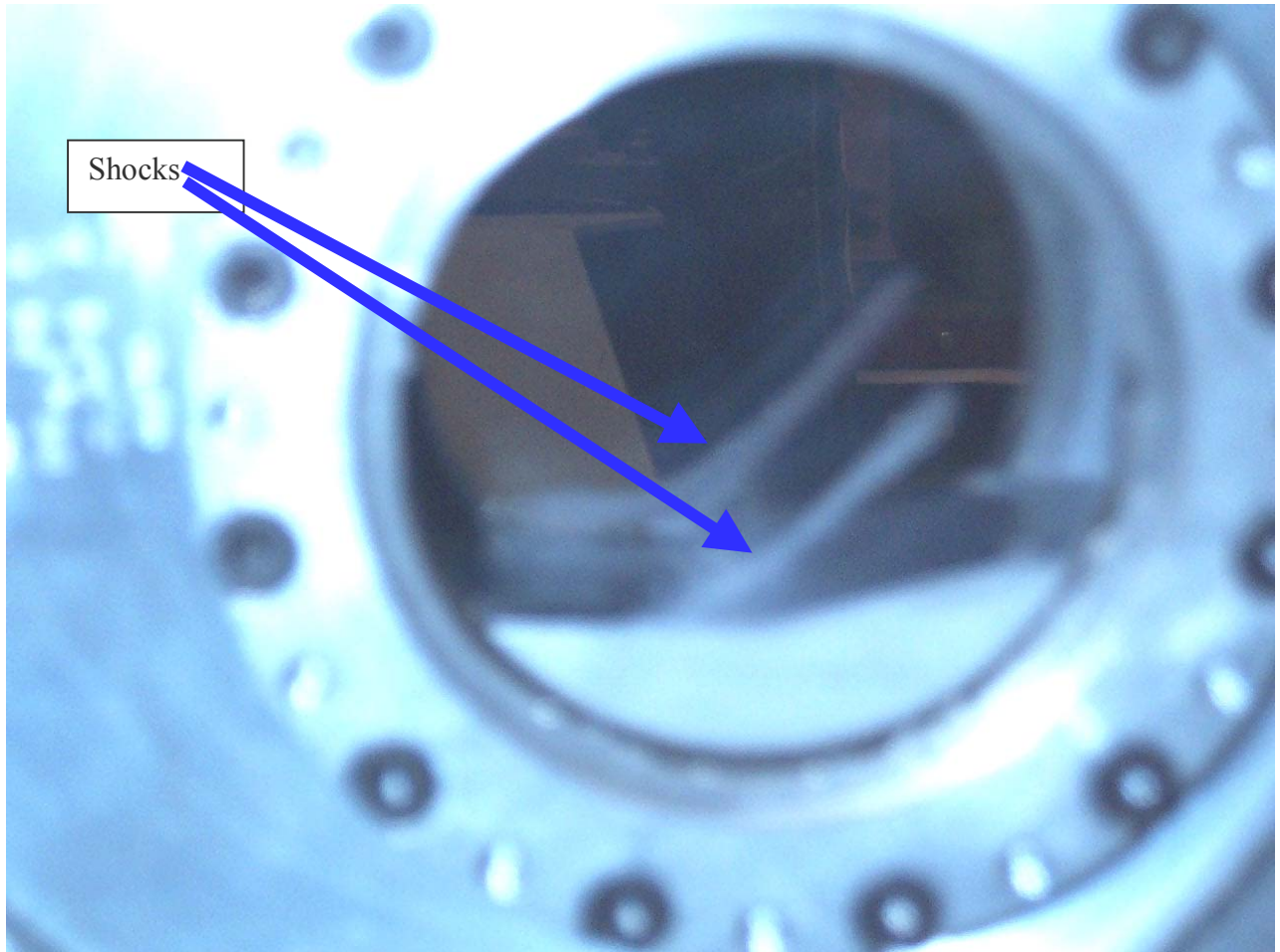
## **Second Day**

### **Oil Flow Visualization**

The second day was started with oil-flow visualization in which paint was placed on a thin film of oil on each of the models as the tunnel was run. The details of this procedure are laid out in the procedure section of this report. The details of the oil flow visualization are found in the pictures taken of the oil-flow visualization.

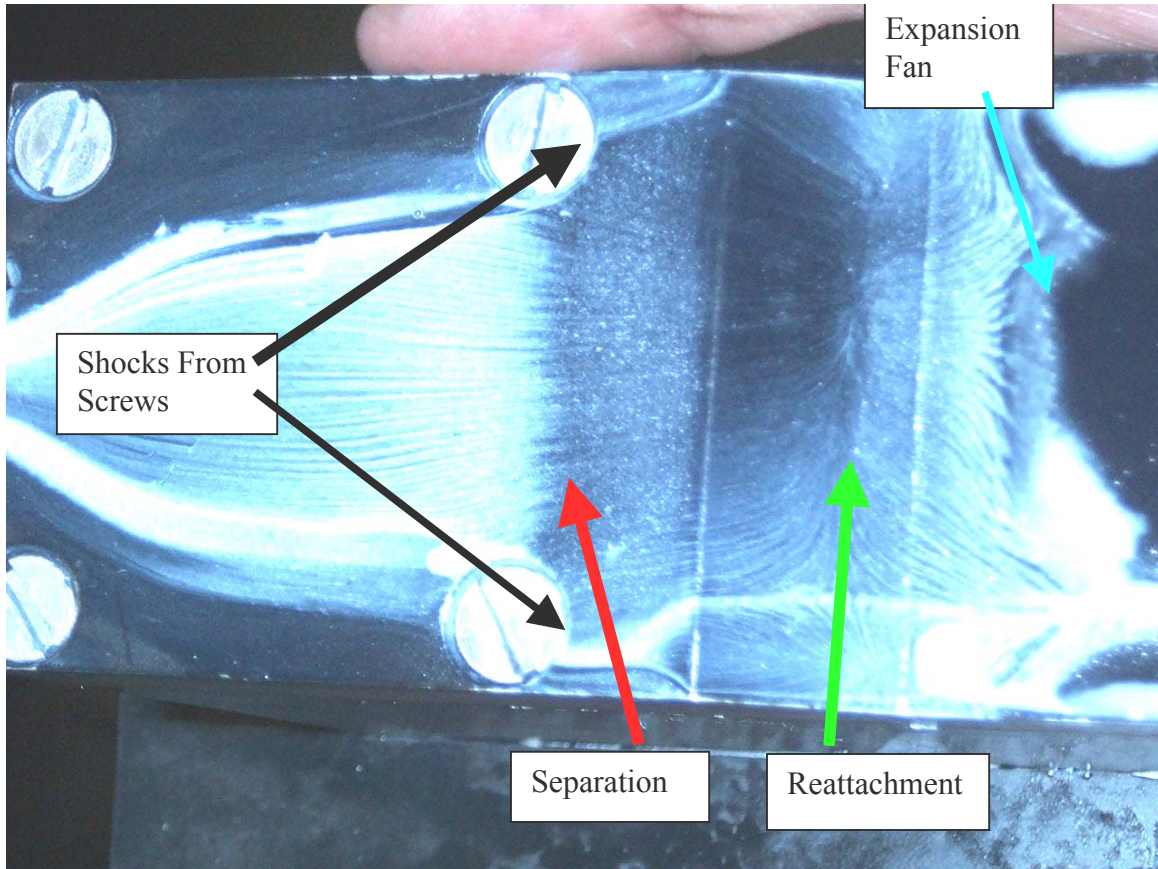
The first pictures were taken of the 15 degree ramps:



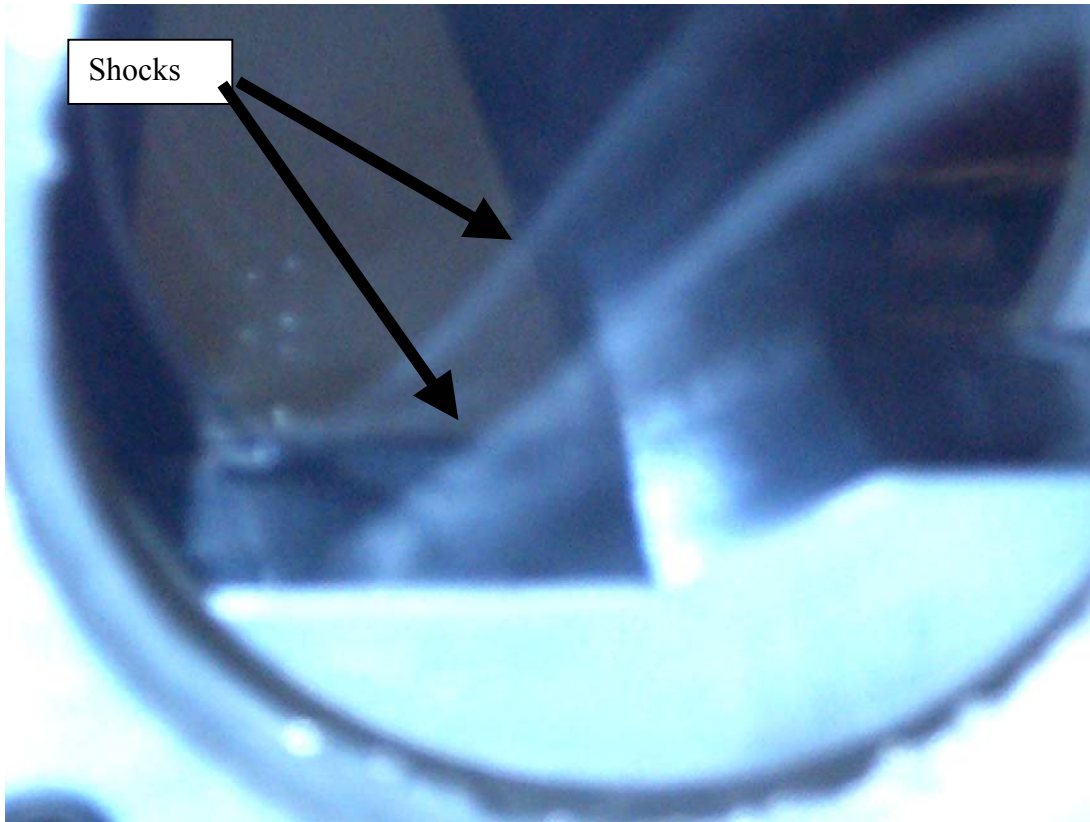


The Shocks are visible in the oil flow, both on the sides of the wind tunnel and on the model itself. The separation bubble is also visible on the model as well as the disturbance from the screws on the model and the expansion fan. The disturbances from the screws may in fact be causing the separation bubble to form earlier than it would if the model were clean.

The following pictures were of the 25 degree ramp:



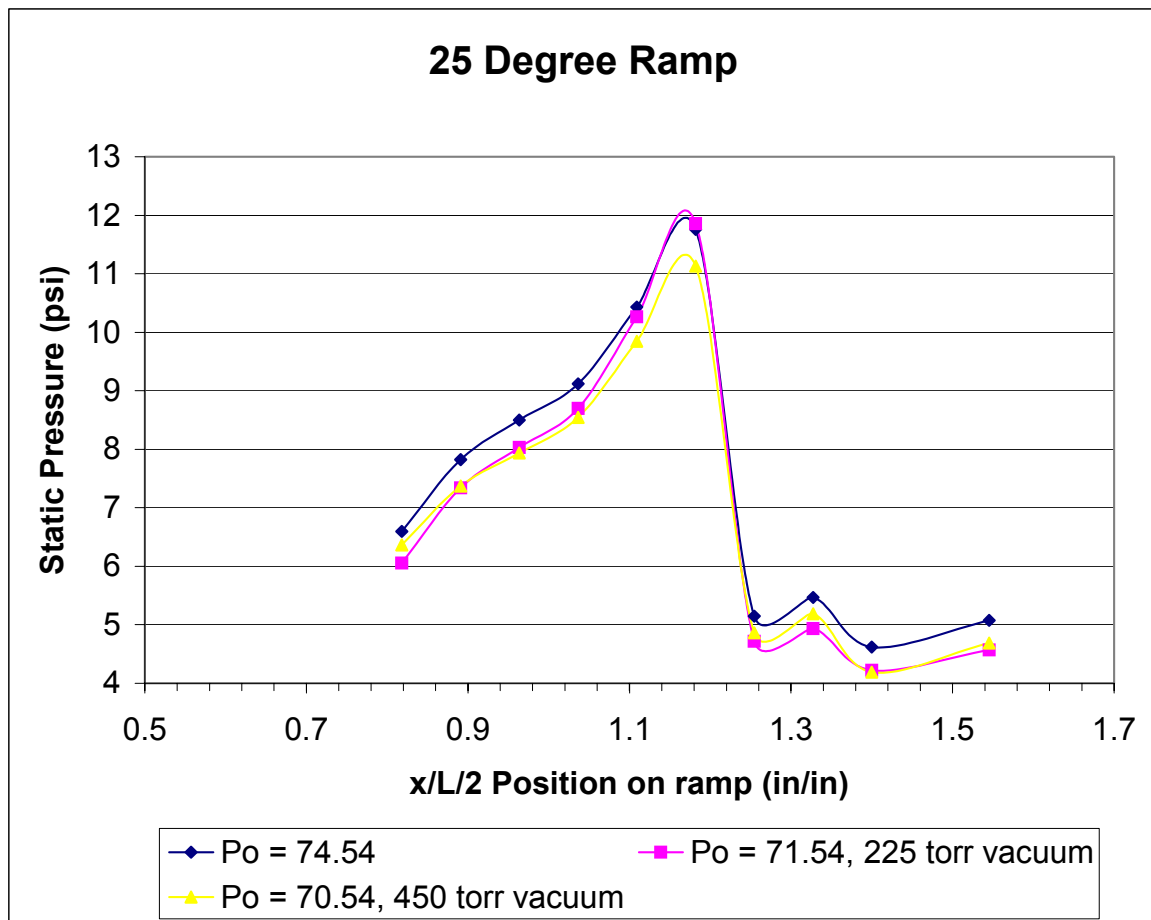




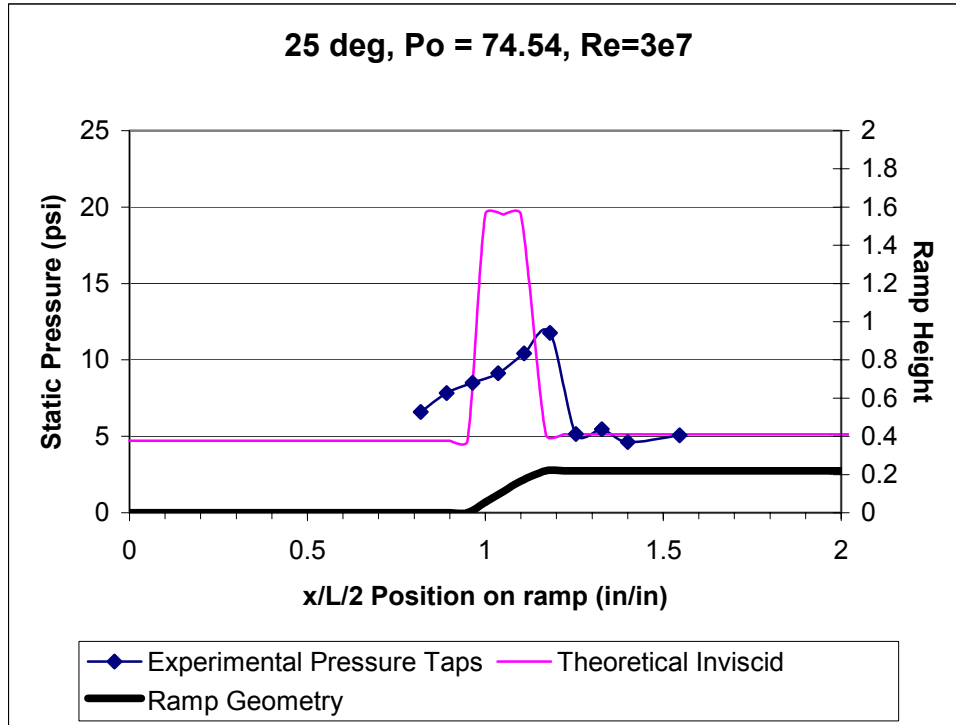
The shocks can also be seen on the 25-degree ramp as they were on the 15-degree ramp, both on the model and on the glass. The incredible size of the separation bubble can also be observed with the oil-flow on the model itself. It seems as if on this model that the screws are influencing the flow in a large way.

**Pressure tap analysis****25-degree ramp**

There were three runs made for each ramp angle with the pressure taps concentrated around the ramp area in order to get better resolution around the shock and expansion areas. Unfortunately the size of the separation bubble was under-estimated and the first pressure taps were in the disturbed flow and thus the lab group was forced to estimate the free-stream Mach number. The tunnel was run with three different plenum pressures of 71 psi, 72 psi, and 75 psi. The three are compared below in the following figure:



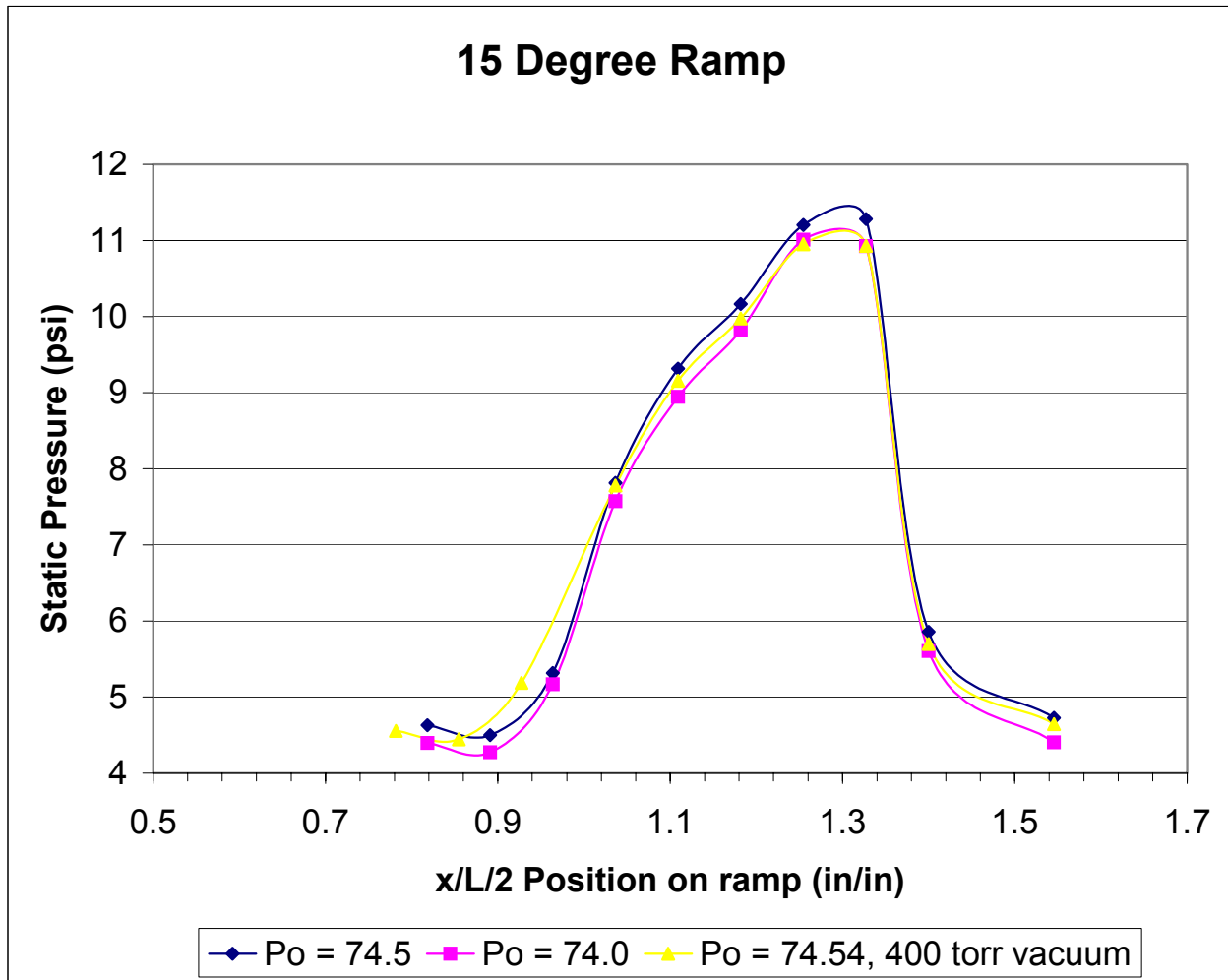
The weakness in this data can be seen in the high-static pressure of the first data point, showing it being already within the first shock and separation bubble. The following figure shows the 75 psi run compared to a theoretical shock event.



As can be observed, the greater resolution of the pressure taps has revealed that though the theoretical functions work okay before and after the ramp, they do not appear to agree with what is happening within the shock region and separation bubble.

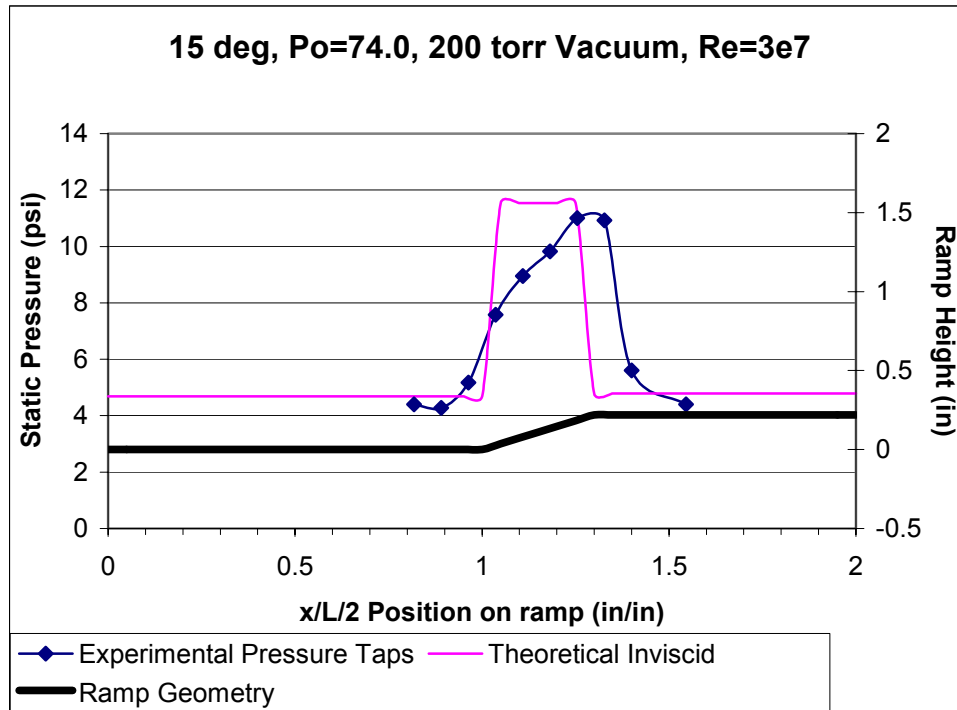
### 15-degree ramp

The 15 degree ramp was analyzed as well with the following chart showing the comparison between the three runs that were made on the second day of 74 psi, 75 psi, and 75 psi with a vacuum exhaust.



As can be seen each run was effectively the same, so a comparison made with one is practically a comparison with all of them. The following chart compares the theoretical static pressure and the actual static pressure on the model for the 74 psi run.





As can be seen in the above graph, the 15 degree ramp follows the theory much more closely, although the pressure rise and plateau seem more gradual. The gradual nature is most probably caused by the separation bubble near the beginning of the compression corner. Once again, though, the theory appears to be right in the global sense, though it falls apart in the local area surrounding the shock.

## **Conclusion and Discussion**

### **Conclusions**

The student lab team was unable to approximate the actual pressure and Mach data from the supersonic tunnel any better than the theoretical approach was able to. The theoretical data appears to match the best to the collected data beyond any of the other analysis available. Additionally it can be concluded from the large errors of the theoretical with the 25-degree ramp that as the ramp angle increases the fidelity of the theoretical model decreases. The 15-degree angle ramp showed a smaller but still significant difference from the theoretical, thus indicating that as the ramp angle decreases, the fidelity of the theoretical model will increase. A further analysis of more ramp angles will be necessary in order to find at what point the differences become negligible.

The Schlieren images proved to be useful in modeling the early flow in the separated region. Unfortunately the image was not sharp enough to detect the smaller shocks and expansion fans that were present around the separated region. A sharper image may be more useful in the exact modeling of the flow in and around the separated region. The Schlieren images still proved a useful tool in analyzing the flow around the compression corner.

The oil-flow visualization proved how large the separation bubble was on the 25-degree ramp and how much smaller the bubble was on the 15-degree ramp. Additionally the oil-flow indicated the extent to which the screws in the surface of the models influenced the flow around the corner and in the separation bubble, especially on the 25-degree ramp. The oil-flow may have also been used to measure the actual size of the shock and separation and probably could have proved useful to make sure that the lab team used pressure taps for collecting data outside the shock and separation area. Oil-flow visualization could be used in further experiments to find things in the tunnel causing shocks and disturbances in the flow.

The primary purpose of this lab was to teach the lab team how to gather data and work with a supersonic wind tunnel. The additional purpose was to allow the students to learn and use various tools for analyzing the flow in a supersonic wind tunnel. The students were able to put together a significant level of analysis and data using practically all the available tools at their disposal. The final conclusion is that the primary purpose of the lab was a success.

### **Limitations**

There were several limitations of the data. In day one, more variation of the pressure tap placement could have seen a little better resolution in the shock and boundary layer area while not losing the cleaner flow near the beginning of the model. There also could have been more runs performed on the original pressure tap placement on the tunnel itself.

The lab team was confused on the use of the vacuum pressure for exhaust, and missed an excellent opportunity to run the tunnel at very low Reynolds number. Also the team never ran the tunnel to sub-sonic speeds.

AAE 520L  
Lab Team 6  
3/15/2004

More data could have been collected on the side-pressure taps but never was.

The lab team did not fully utilize the data provided by the flow visualization on the second day. This would have allowed the pressure tap data to include points outside the disturbed flow.

### **Error Analysis**

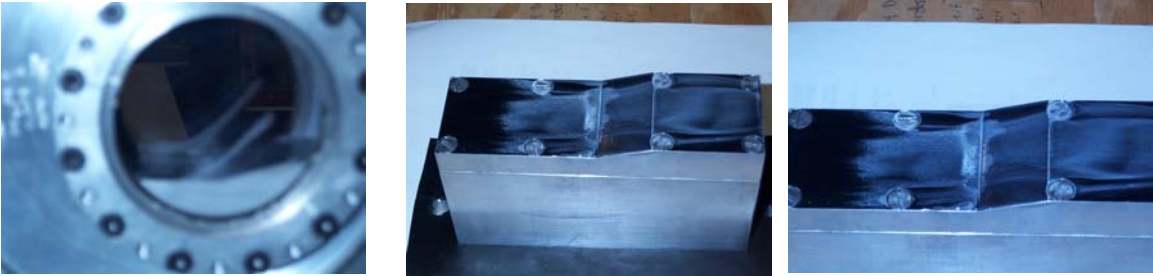
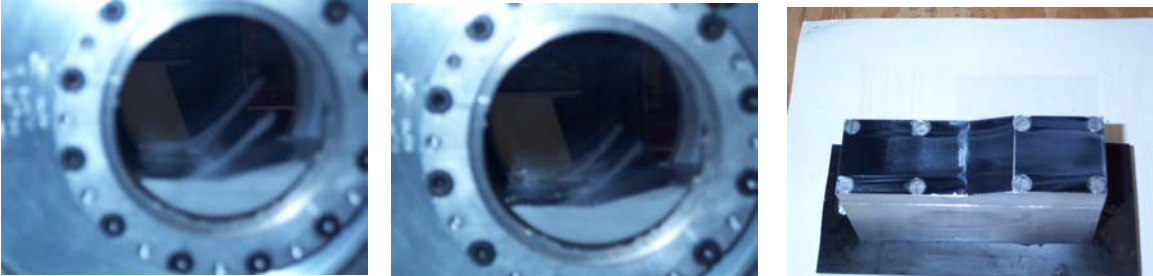


Most of the data was qualitative in this test, although a further analysis of the numerical difference between the theoretical and actual is warranted.

AAE 520L  
Lab Team 6  
3/15/2004

## ***References***

“A & AE 520 Background Information, Adapted from AAE334L” 19-Jan-04. Purdue University, West Lafayette, IN.  
Barlow, Jewel B., Rae, W.H., Pope, A., “Properties of Air and Water”, Low-Speed Wind Tunnel Testing, 3<sup>rd</sup> ed., John Wiley & Sons, New York, NY, 1999, pp.7-9.

Appendix

<u>Temp</u> <u>deg C</u>	<u>Heise(psi</u> <u>gauge)</u>	<u>Ramp</u> <u>(deg)</u>	<u>Vacuum</u> <u>(torr)</u>	<u>Re</u>	<u>Theoretical Shock</u> <u>angle</u>
18.8	50	15		2.65E+07	37
					
18.4	57	15		2.94E+07	37
					
18.4	61	15		3.10E+07	37
					
19	59.5	15	150	3.03E+07	37
					

AAE 520L  
Lab Team 6  
3/15/2004

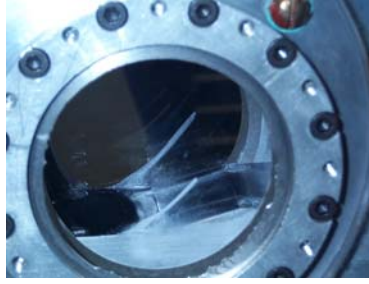
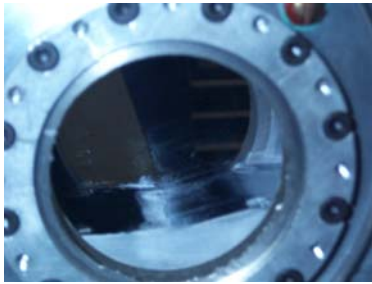
16

57

25

$2.97\text{E}+07$

50



16

60

25

$3.09\text{E}+09$

50



18.4

60

25

$3.06\text{E}+07$

50



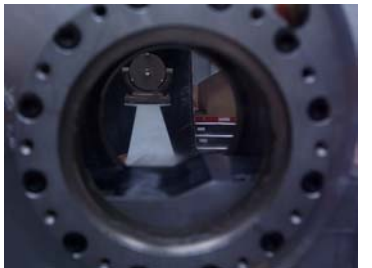
18.2

61

25

$3.11\text{E}+07$

50



AAE 520L  
Lab Team 6  
3/15/2004  
18.8

60

25

200 3.06E+07

50

